A Novel Chitosan-Based Fluorescence Chemosensor for Selective Detection of Fe (III) Ion in Acetic Aqueous Medium

Mehrad Pournaki

Submitted to the
Institute of Graduate Studies and Research
in partial fulfillment of the requirements for the degree of

Doctor of Philosophy
in
Chemistry

Eastern Mediterranean University
February 2021
Gazimağusa, North Cyprus

Approval of the Institute of Graduate Studies and Research

Prof. Dr. Ali Hakan Ulusoy
Director

I certify that this thesis satisfies all the requirements as a thesis for the degree of Doctor of Philosophy in Chemistry.

Prof. Dr. İzzet Sakallı
Chair, Department of Chemistry

We certify that we have read this thesis and that in our opinion it is fully adequate in scope and quality as a thesis for the degree of Doctor of Philosophy in Chemistry.

Assoc. Prof. Dr. Hayrettin Ozan Gülcan
Co-Supervisor

Prof. Dr. Mustafa Gazi
Supervisor

Examining Committee

1. Prof. Dr. Murat Ateş
2. Prof. Dr. Mustafa Gazi
3. Prof. Dr. Okan Sirkecioğlu
4. Prof. Dr. Osman Yılmaz
5. Asst. Prof. Dr. Aybike Yektaoğlu

ABSTRACT

An ecofriendly chitosan-based urolithin fluorescence (Uro-*m*-Ch) optical sensor was successfully synthesized and characterized by Fourier transform infrared spectroscopy. According to the FTIR results, the chitosan characteristic peaks were observed around 3500−3300 cm^{-1}, 1656 cm^{-1}, 1587 cm^{-1} and 1179 cm^{-1} which are attributed to hydroxyl, amide I, N–H deformation and C–O–C stretching, respectively. The Uro-*m*-Ch featured the representative peaks of chitosan and the lactone carbonyl stretching of the urolithin. The Uro-*m*-Ch demonstrated fluorescence character in the presence of 1% (v/v) CH_3COOH/H_2O solution with a maximum excitation wavelength (λ_{max}) within 290–330 nm and λ_{max} emission spectrum at 430 nm with Stokes shift of 100 nm without the target metal ion. Notably, in the presence of iron (III) concentration from 0.10 to 0.080 mM; Uro-*m*-Ch exhibited a maximum wavelength emission at 420 nm with a decreasing trend in fluorescence intensity. During the selectivity and interference studies, Uro-*m*-Ch demonstrated a remarkable quenching effect only with Fe^{3+} ion among various mono- and multivalent metal ions. Considering the fluorescence responses of the Uro-*m*-Ch, its sensing mechanism towards Fe^{3+} ion was attributed to intramolecular energy/electron transfer between the lactone group of the urolithin and/or the hydroxyl moiety of the chitosan backbone and the iron (III) ion. Results herein confirmed that Uro-*m*-Ch is rapid, selective and sensitive towards Fe^{3+} ion detection in aqueous acetic solution.

Keywords: Chitosan, Urolithin B, Iron (III) ion, Fluorescent, Chemosensor, Selective detection

ÖZ

Çevre dostu kitosan bazlı ürolitin floresan (Uro-*m*-Ch) optik sensör başarıyla sentezlendi ve Fourier dönüşümü kızılötesi spektroskopisi ile karakterize edildi. FTIR sonuçlarına göre, kitosanın karakteristik zirveleri olan hidroksil, amid I, N–H deformasyonu ve C–O–C uzaması sırasıyla 3500−3300 cm^{-1}, 1656 cm^{-1}, 1587 cm^{-1} ve 1179 cm^{-1} dalga numaralarında gözlenmiştir. Uro-*m*-Ch, kitosanın temsili zirvelerine ve ürolitinin lakton karbonil gerilmesine sahipti. Uro-*m*-Ch, %1 (v/v) CH_3COOH/H_2O çözeltisinin varlığında 290-330 nm arası maksimum uyarma dalga boyu (λ_{max}) ve hedef metal iyonu yokluğunda 100 nm Stokes kayması ile 430 nm'de λ_{max} emisyon spektrumu olan bir floresan karakter sergilemiştir. Özellikle, 0.10 ila 0.080 mM arasında demir (III) konsantrasyonunun varlığında; Uro-*m*-Ch, floresan yoğunluğunda azalan bir trendle 420 nm'de maksimum dalga boyu emisyonu sergiledi. Seçicilik ve engelleme çalışmaları sırasında, Uro-*m*-Ch, çeşitli tek ve çok değerlikli metal iyonları arasında yalnızca Fe^{3+} iyonu ile dikkate değer bir söndürme etkisi göstermiştir. Uro-*m*-Ch'nin floresan tepkileri göz önüne alındığında, Fe^{3+} iyonuna yönelik algılama mekanizması, ürolitinin lakton grubu ve / veya kitosan omurgasının hidroksil kısmı ile demir (III) iyonu arasındaki molekül içi enerji / elektron transferine atfedildi. Buradaki sonuçlar, Uro-*m*-Ch'nin hızlı, seçici ve sulu asetik çözelti içinde Fe^{3+} iyonu tespitine karşı duyarlı olduğunu doğruladı.

Anahtar Kelimeler: Kitosan, Ürolitin B, Demir (III) iyonu, Floresan, Kemosensör, Seçici tespit

ACKNOWLEDGMENT

I am very pleased to express my sincere gratitude and to thank my wonderful parents, Mr. Mohammad Hasan Pournaki, Mrs. Shahla Rezaie and my brother. I would not have come into this world without their blessings or had this excellent opportunity to undergo valuable academic pursuit.

I would like to express my sincere gratitude to Prof. Dr. Mustafa Gazi, my advisor, for his support during my studies. I was constantly driven by his patience, inspiration, excitement, and immense knowledge of my subject while I was doing my research and writing this thesis. I couldn't have dreamed of a better mentor and counselor. I also greatly appreciate Assoc. Prof. Dr. Hayrettin Ozan Gülcan, particularly for his willingness to share his expertise in the synthesis of the sample compounds and his dedication to his position as my co-supervisor. In addition to my advisors, I would like to thank the members of the thesis committee for their critical reviews, motivation, informative remarks, and professional recommendations to further develop my doctoral thesis.

Lastly, I wish to express my deep sense of appreciation and respect to the members of the Pharmacy Faculty for their competent support and encouragement through my studies and research work. To all of you, I am eternally thankful: Prof. Dr. Müberra Koşar, Prof. Dr. Mustafa Fethi Şahin, Prof. Dr. Gönül Şahin, Prof. Dr. Emre Hamurtekin, Assoc. Prof. Dr. Hayrettin Ozan Gülcan, Assist. Prof. Dr. Aybike Yektaoğlu, Assist. Prof. Dr. Emine Vildan Burgaz, Assist. Prof. Dr. Hasip Cem Özyurt Assist. Prof. Dr. İmge Kunter, Assist. Prof. Dr. Jale Yüzügülen, Assist. Prof. Dr.

Mehmet İlktaç, Assist. Prof. Dr. Tuğba Erçetin, Sr. Instr. Canan Gülcan, Sr. Instr. Emine Dilek Özyılmaz, Sr. Instr. Leyla Beba Pojarani. Sr. Instr. Mustafa Akpınar, Emine Alpsoy Ertoprak, Mehmet Kumral, Şima Kubilay and Osman Şıh Veysel,

TABLE OF CONTENTS

LIST OF TABLES

LIST OF FIGURES

LIST OF SYMBOLS AND ABBREVIATIONS

EET	Electronic Energy Transfer
FRET	Fluorescence Resonance Energy Transfer
FTIR	Fourier-transform infrared spectroscopy
HOMO	Highest occupied molecular orbital
ICT	Intramolecular Charge Transfer
LUMO	Lowest un-occupied molecular orbital
L-Cys	L-cysteine capped
PCT	Photo-induced Electron Transfer
PET	Photoinduced Electron Transfer
TLC	Thin Layer Chromatography
Uro-Cl	3-(3-chloropropoxy)-6H-benzo[c]chromen-6-one
Uro-*m*-Ch	Urolithin modified Chitosan
Urolithin A	(3,8-dihydroxybenzo[c]chromen-6-one)
Urolithin B	(3-hydoxybenzo[c]chromen-6-one)
μM:	Micro Molar

Chapter 1

INTRODUCTION

Heavy metal contamination of water and soil is becoming one of the most severe environmental concerns worldwide, even at trace levels owing to their toxicity and biological persistence [1]. With the rapid growth of industries, effluents containing metal ions are increasingly discharged directly or indirectly into the atmosphere. While some of these heavy metals (i.e, iron, cobalt, or zinc) are critical nutrients, they can be toxic at higher concentrations [1–3].

For instance, iron plays a range of physiological functions within the body system, such as oxygen digestion mechanism, muscle withdrawal, nerve conduction, acid-base direction and osmotic pressure adjustment in cells [3–5]. However, excess iron content can be disastrous because it's can easily initiate various redox reactions within the human body which may results in carcinogenic or nervous disorders, among other diseases [4]. While the Environmental Protection Agency's maximum amount of iron (III) ion allowed in drinking water is 5.4 μmol L^{-1} [4], higher concentration has been frequently detected in water streams [4,5].

Notably, at trace amounts; cadmium, lead, and mercury are extremely toxic, constituting a close connection with neurodegenerative diseases [6]. Unlike organic contaminants that can be degraded, trace metals remain permanent in sediment environments, where they can pose serious toxicity threats to benthic and aquatic species [1–6]. The scientific community has been stimulated in recent years by the development of highly selective and fast-response probes for the detection of various pollutants in the face of increasingly stringent environmental regulations. This PhD research is aimed at contributing to key knowledge gaps in rapid sensing of commonly detected heavy metal ions in the aqueous environment.

Several techniques for Fe^{3+} detection; such as mass spectrometry, atomic absorption spectroscopy, electrochemical analysis and colourimetric analysis, have been developed [7–11]. Even though these techniques have demonstrated different degrees of effectiveness, however, high-cost, complicated and technical difficulties, excessive reagents use are some of their many drawbacks [12–15]. Fluorescence-based sensing technology offers significant advantages of easy operation, instant/fast response, technical simplicity, high selectivity and high sensitivity, among the various optical sensors for heavy metal ion detection [16–25].

It is worth noting that detection at low concentrations of heavy metal ions is a priority for the protection of the environment and the prevention of diseases. Although, these heavy metal ions are difficult to sense in aqueous media due to various influencing factors like high hydration, pH-influenced speciation among many others. Also, note that the paramagnetism nature of iron ions quenching the fluorescence of many fluorophores complicate its analysis. As a result, when developing selective fluorescent probe for bioenvironmental applications, these limits must be taken into account.

To date, a number of fluorescent probes with various recognition/binding mechanisms have been developed for the detection of Fe^{3+} ions [10–35]. The successful Fe^{3+}

fluorescent chemosensors are majorly restricted to quantum dots, fluorescent organic molecules, and their complexes. However, these organic molecules often involve complicated synthesis route and their complexes may exhibit poor photostability [22–30].

Therefore, developing appropriately photostable and environmental friendly chemosensors for detecting Fe^{3+} ions in various aqueous systems is still a worthwhile and challenging scientific task. In this PhD study; a natural coumarin compound, a urolithin derivative was modified biopolymeric chitosan and applied as a potent environmentally friendly and stable Fe^{3+} ions selective fluorescent probe in a multipollutant matrix.

1.1 Chemosensors

A chemosensor contains molecule structure(s) (organic or inorganic complexes) which interacts with analytes to produce a detectable change with a specific analyte, hence, often called a molecular sensor [20–27]. The use of chemosensors is referred to as chemosensing and maybe an electrochemically or optically based system. The chemosensors are designed to contain a mode of signaling and recognition that is connected either directly to each other or through a connector or spacer [20–28].

The signaling moiety or receptor site acts as a signal transducer, producing changes *via* either (or both) the visible and ultraviolet absorption or the emission property [30–40]. Consequently, according to the nature of the signal produced by the signaling subunit, chemosensors are classified into three categories; (***a***) colourimetric sensors associated with changes in electronic properties leading to visible colour changes (***b***) fluorogenic sensors associated with excited and photo-induced electron transfer mechanisms and (***c***) electrochemical sensors associated with the measurement of changes in redox potential [41].

The recognition moiety is responsible for binding to the analyte selectively and reversibly; which is dependent on the characteristics of the target (a charge, and radius, coordination number and size of the molecule, etc.) and the nature of the solvent (ionic strength, polarity and pH) [20–41]. Figure 1 shows a schematic representation of a chemosensor consisting of a signaling moiety and a mode of recognition that are linked together to facilitate communication between the two components.

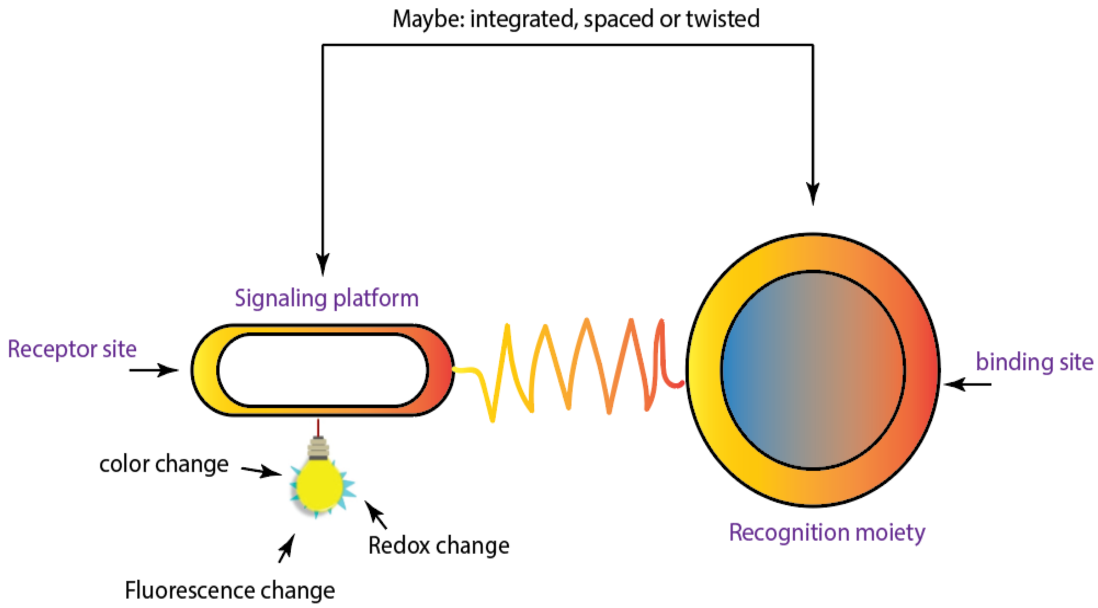

Figure 1: Schematic illustration of a typical chemosensor [41]

1.1.1 Colourimetric chemosensing

Colourimetric sensors are a class of optical sensors that, when influenced by external stimuli, alter their colour. Any shift in the physical or chemical environment can be seen as a stimulus of this kind [25]. Colourimetric chemosensors (signal recorded using ultraviolet-visible spectroscopy) induces changes in their absorption properties, such as in absorption wavelength, intensity strength or chirality [26].

Compared to fluorescence-based analytical methods; colourimetric chemosensors are relatively simple to use as it depends on colour variations that might be apparent to the naked eye. For example; He et al. [42] synthesized novel gold nanoparticles based colourimetric chemosensor to measure phosphate concentration. The observed colour change of the probe was reportedly activated by the affinity between the Zn^{2+} ion complexed in the probe and the phosphate ion. Recently, Chen et al. [43] reported a phosphate ion based colourimetric probe that changes colour based on the rapid interaction between the TiO_2 recognition nanotube and the target phosphate ion; and resulted in the lowest limit of detection of 0.59 μM and linear range from 1 μM to 40 μM.

1.1.2 Fluorescent chemosensing

Fluorescence is a relaxation process based on radiative spin-allowed mechanism in which the excited (G_1) and ground states (G_0) have the same multiplicity. As a result, it happens on relatively short timescales, probably in the picoseconds to microseconds range. The Perrin-Jablonski diagram (shown in Figure 2) is useful for easily visualizing the most common processes that occur after photon absorption [44,45].

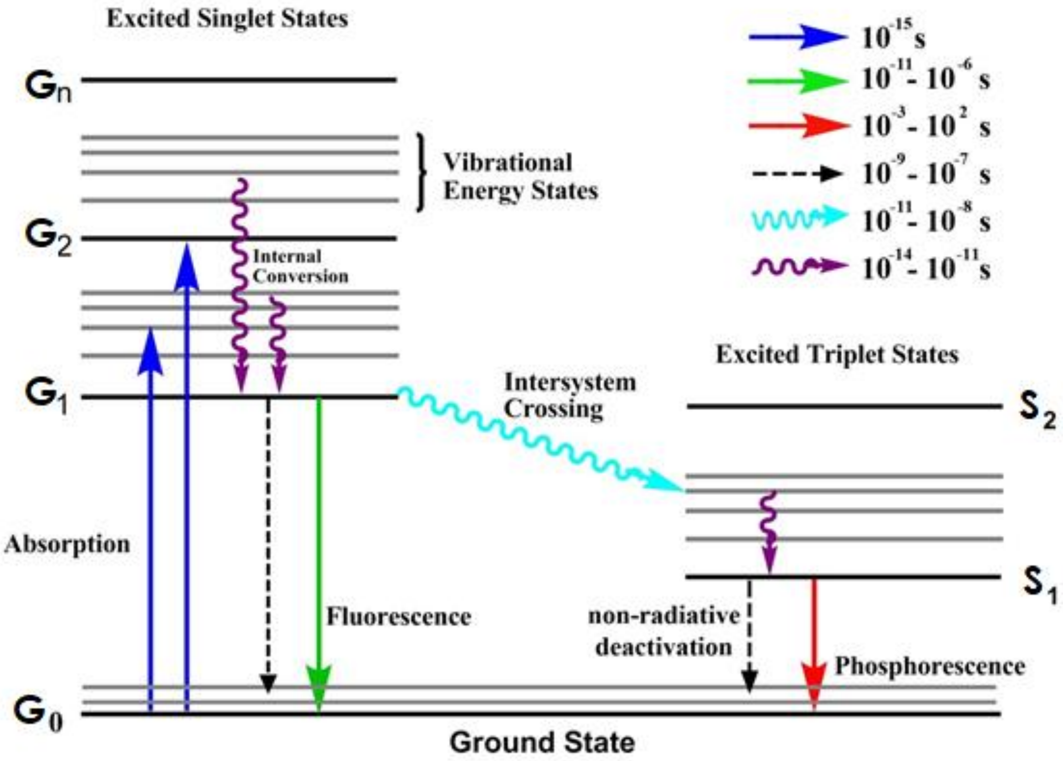

Figure 2: Perrin-Jablonski diagram showing fluorescence and phosphorescence [3].

Following light absorption, the vibrational levels of some of the upper excited states will be populated with electrons. These electrons instantly relax to G_1 by vibrational relaxation in picoseconds or less and at this stage, all other photochemical processes have a better chance of occurring [45].

As seen in the Jablonski diagram, absorbed light has a shorter wavelength than the emitted light due to minimal energy loss by the molecule prior to absorption. Stokes shift is the difference between the spectral positions of absorption and luminescence band maxima (see Figure 3). Fast decay of the excited electrons via non-radiative pathway is the key cause of Stokes shift. In addition to this effect, due to other photon-initiated reactions, fluorescent molecules may show additional Stokes shift [44,45].

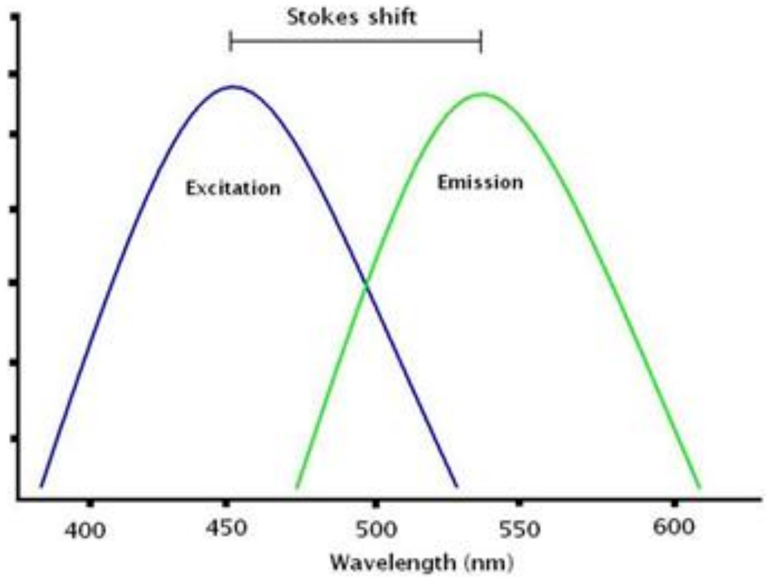

Figure 3: Stokes shift in fluorescence spectroscopy [45].

An active area of research is fluorescence sensing of various toxic and emerging analytes. The need to reduce the use of costly radioactive tracers for use and disposal motivates these efforts. For a broad range of clinical, bioprocess, and environmental applications, fast and low-cost testing methods are needed [29,32, 36]. Fluorescent chemosensors are detection devices or probes that contain compounds with a binding molecule, a fluorophore (signaling moieties), and a mechanism for making contact between the components [24–26].

Generally, fluorescent chemosensors working theory involves the emission of light after being excited at lower wavelengths by a substance (fluorophore). That emission's intensity varies with the target analyte's concentration [20–25]. Fluorescent chemosensor analyte detection is typically achieved through varieties of photophysical mechanisms, including emission induced aggregation; enhanced fluorescence induced chelation; photoinduced electron transfer; intramolecular charge transfers etc., [29]. Covalent [22–23] and non-covalent [24] bonds can be used to bind analytes. Metal chelation, hydrogen bonding, π–cation complexation, electrostatic attraction, or π–π interactions are all examples of non-covalent interactions between receptor and analyte [24, 27].

The visible changes during the binding process may be due to enhancement of the fluorescent signal, quenching or shifts in the emission wavelength of the fluorophores [29]. The common types of fluorescent chemosensors are the one having a spacer between the fluorophore and the receptor as shown in Figure 4 while the second type as no spacer which is an integrated configuration system [46–50] is shown in Figure 5.

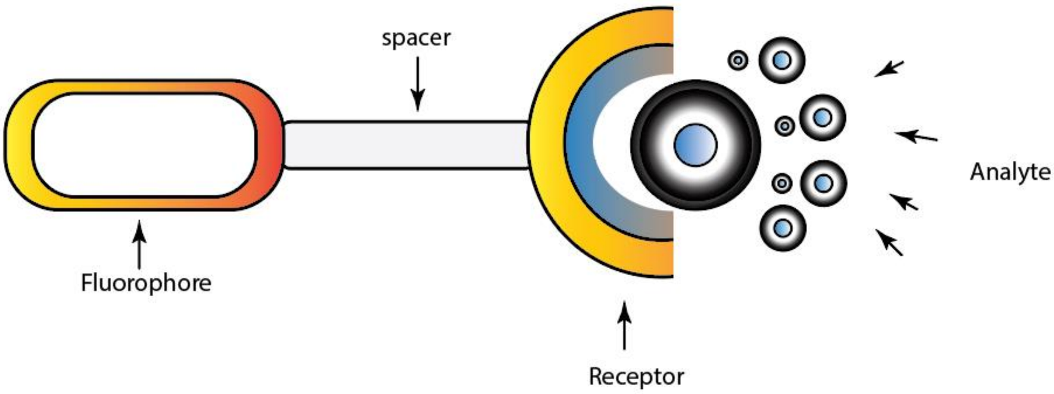

Figure 4: A probe containing receptor and spacer as a unit

As shown in Figure 5, there is an electrical conjugation between the receptor and the fluorophore in the fluorescent probe based on integrated configuration.

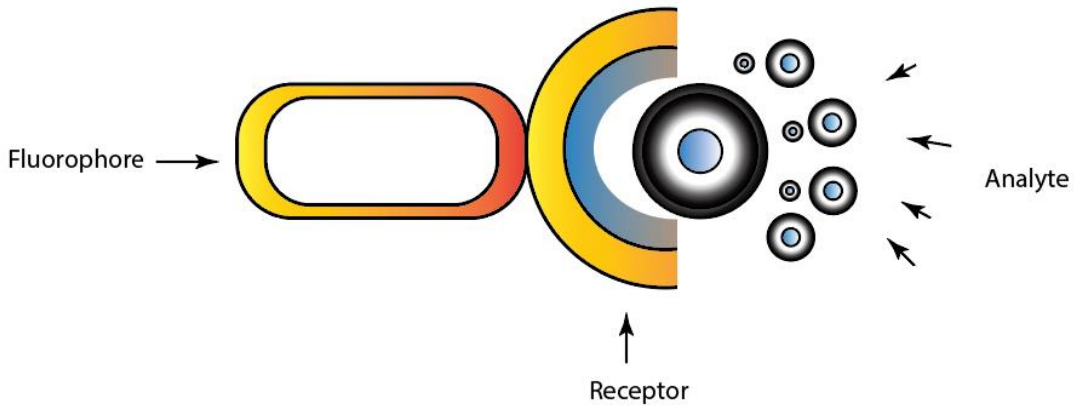

Figure 5: An integrated fluorescence chemosensor.

Various fluorophores and binding molecules have been developed and reported for fluorescence chemosensors with varying degree of success. For instance; Li et al. [51] developed an L-cysteine capped iron oxide modified zinc oxide probe for sensing Fe^{3+} in aqueous media. They believed that the nanoprobe had excellent fluorescent properties and remarkable selectivity for Fe^{3+}, which they attributed to L-Cys' strong attachment to Fe^{3+}, which notably decreased the fluorescence in the pH range of 4.98–7.39.

They reported that nanoprobe demonstrated excellent fluorescent property and high selectivity for Fe^{3+} attributed to the binding affinity of L-Cys with Fe^{3+} which induced an apparent decrease of the fluorescence under a pH range of 4.98–7.39.

Similarly, Arulraj et al. [52] developed a Ag^+ femtomolar sensing probe. They reported that the Ag^+ detection was achieved *via* a static fluorescence quenching with a statistically significant linear relation of $5 \times 10^{-15} - 8 \times 10^{-13}$ M. Various organic (fluorescent) dyes have been used for the development of fluorescence-based sensors due to their attractive characteristics such as high coefficient of molar extinction, ease of alteration, and the presence of several reactive sites in their skeletons [53–60].

These fluorophores are modified with an ion (ionophore) recognition moiety to detect heavy metal ions, which functions as the host for the target metal ions. The interaction between the ionophore and the target analyte produces a change in the fluorophore's photophysical characteristics, which translates into a change in its fluorescent emission, usually from 'off' to on' [56,58]. A rapid Hg^{2+} probe was developed by Li and colleagues [61] based on a rhodamine B derivative linked to an NS_2 unit. They recorded a linear range from up to 1.6×10^{-5} M with a 2.36×10^{-6} M limit of detection. They noted that no competing ions interfered with the probe response to Hg^{2+} in real natural water samples.

1.2 Fluorescence Sensing and Signaling Mechanisms

A wide variety of analytes, such as cations, anions or neutral molecules, are quickly, sensitively and sometimes visually detected by luminescent sensors. Excited molecules can either transfer an electron to a quencher from a potential donor or to fill an empty orbital before relaxing [29–35]. Note that a luminophore may be organic or inorganic and referred to as an atom or group of atoms in a chemical compound that manifests luminescence (responsible for a given emission band when it undergoes luminescence). Luminophores are subcategorized into fluorophores and phosphors [36–43]. The sections below discuss briefly the signaling mechanisms in fluorophore sensing.

1.2.1 Photoinduced Electron Transfer (PET)

PET is an excited state electron transfer mechanism that transfers an excited electron to an acceptor from a donor. Both the luminophore and the receptor are located in the same molecule in the PET-type fluorescence sensor and are bound by a non-conjugated bridge [56–65]. When a photon excites the fluorophore in the PET system, an electron in a ground state orbital is excited to a higher energy orbital. An electron donor will fill a vacancy in a ground state orbital created by this excited state. The fluorophores are in a higher-energy orbital than the vacancy left by the excited electron in the excited state.

The receptors typically have a relatively high-energy lone pair or non-bonding electrons which transited into the lower-energy orbital, then quench the excited fluorophore fluorescence in the absence of analytes, as shown in Figure 6, resulting in "OFF" mechanisms. If the receptor's lone electron pair binds a cation or a proton, the bound pair energy is reduced which inhibits the electron transfer and restricting the quenching of the fluorescence [66–70], as shown in Figure 7 demonstrating the "ON" mechanism.

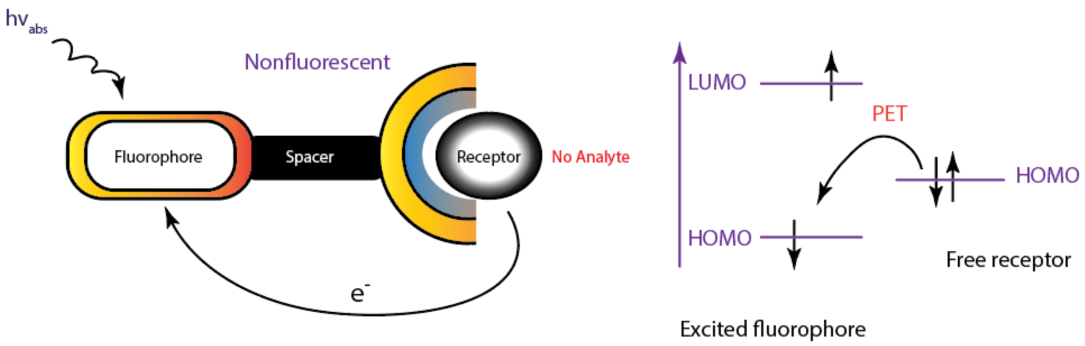

Figure 6: PET mechanism due to fluorescence quenching in the absence of the analytes (“OFF”)

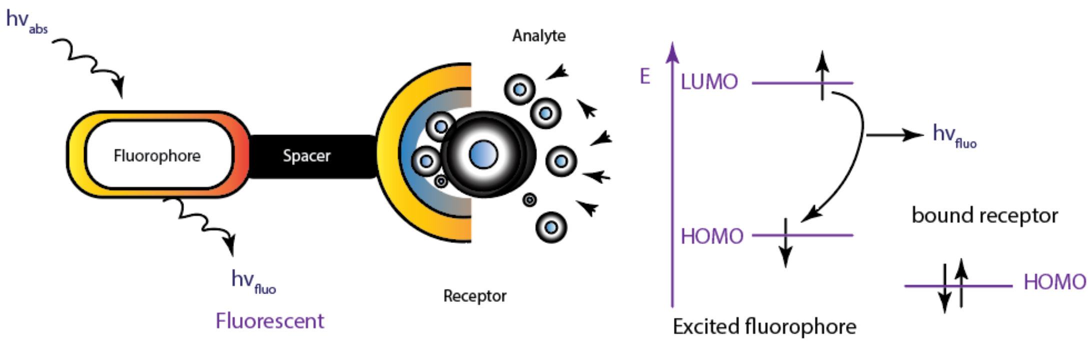

Figure 7: PET mechanism in the presence of analytes without fluorescence quenching ("ON")

The analyte's selectivity is improved by selecting an appropriate binding/recognition material for the target analyte, and some recognition molecules are further functionalized or doped to boost their efficiency. The PET mechanism is demonstrated for Zn^{2+} ions detection in the study reported by Turfan and Akkaya [71]. The fluorophore was a vivid green boradiazaindacene fluorescence, and the receptor was 2,2-bipyridine. According to their results, a PET-based mechanism from the excited state fluorophore to the bipyridyl unit complexed to Zn^{2+} ions quenched the fluorophore. In the absence of Zn^{2+} ions, the fluorophore fluoresced brightly green, but it fluoresced surprisingly weakly when complexed with Zn^{2+} ions, as shown in Figure 8.

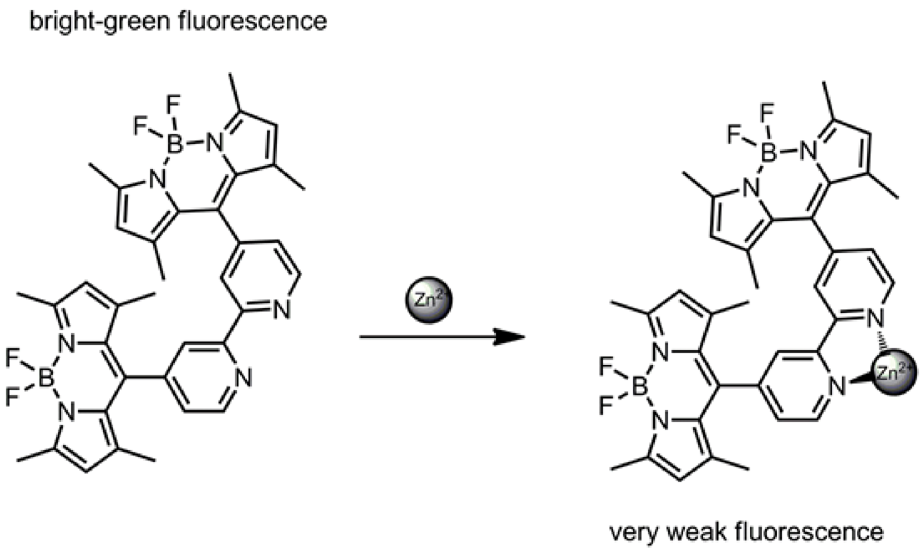

Figure 8: Modulation of fluorescence emission via PET mechanism [71].

1.2.2 Intramolecular Charge Transfer (ICT)

The ICT is an electron transfer process that occurs in molecules that are normally *pi*-conjugated with an electron donor and an electron acceptor connected by a bridge of *pi*-conjugated backbone when they are photoexcited. This kind of signaling mechanism generally results in a shift in the wavelength [72]. Unlike PET-type chemosensors, the ICT sensor has no spacer unit between the receptor and fluorophore. An illustration of the ICT-based fluorescence signaling mechanism is demonstrated in Figure 9 where the receptor unit contains an electron donor which in this case is aniline and receptor which contains electron acceptor which in this case is pyridine exhibiting opposite spectral shifts upon protonation.

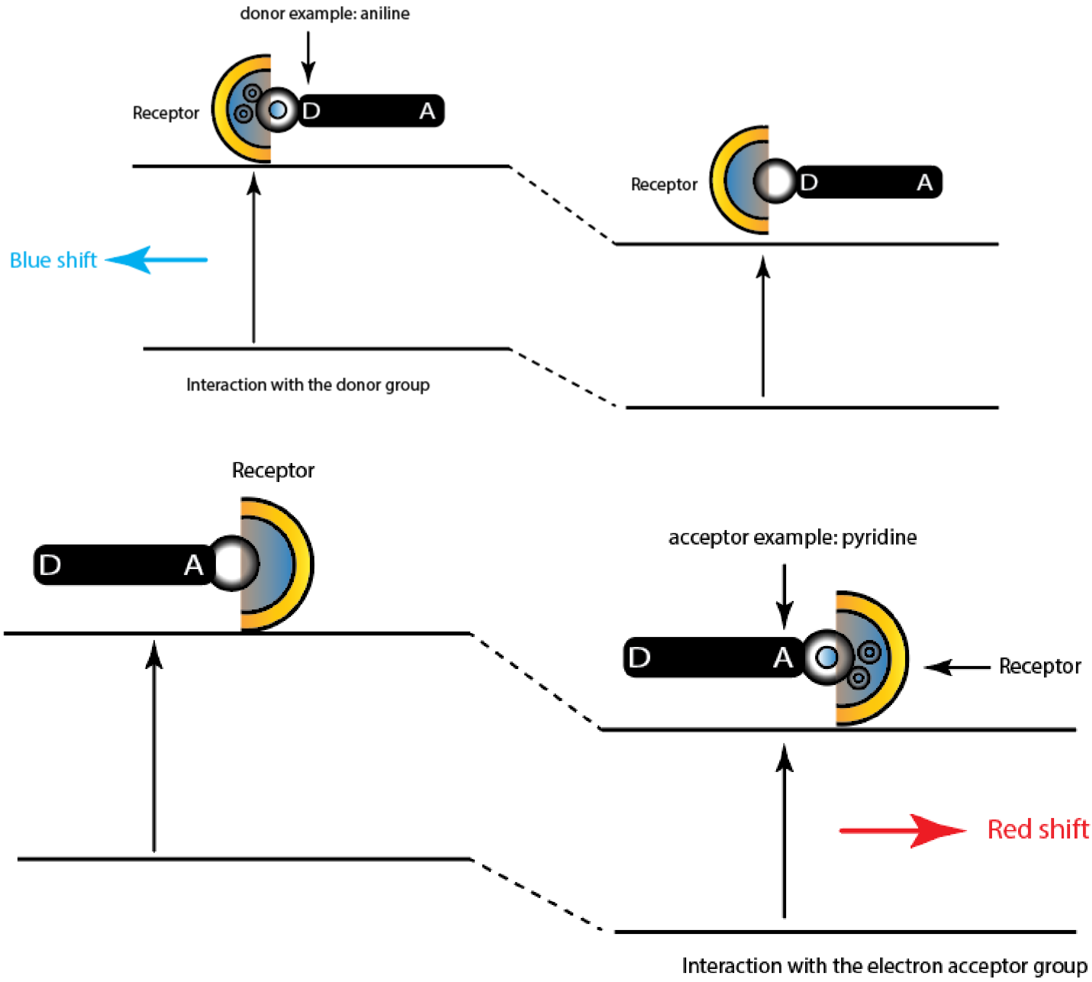

Figure 9: Spectral shifts of ICT-based fluorescence sensors

Here, the receptor unit is attached to the π-electron unit of the fluorophore, which has two electron terminals, one of which is an acceptor and the second one is a donor [72,73]. In the ICT system, a redistribution of electron density takes place when the receptor-fluorophore component absorbs photons and get excited to produce dipoles. This causes the transition of internal charges to the acceptor from the donor when the analyte interacts with the dipoles of the excited fluorophores [73].

The ICT-based phenothiazine fluorescent probe was reported by Kaur et al. [74] in 2016 for selective sensing of Cu^{2+} and Hg^{2+} ions. After Cu^{2+} ion was introduced into the system, a noticeable change in the colour to blackish-blue from orange was observed. The binding mechanism was based on interactions between sulfur and nitrogen atoms of the phenothiazine-based probe and the target Cu^{2+} ions, according to the authors. This interaction produced a decrease in the electron density, which caused the fluorescence to be quenched.

1.2.3 Energy Transfer (ET)

Energy transfer is a signaling process in fluorescence sensing that can be defined as fluorescence resonance energy transfer or electronic energy transfer depending on the contact distance between the participating units (energy donor and receiver receptor) inside the fluorophore-binding unit systems [73]. The donor which is represented as **D** (Figure 10) absorbs light at a short wavelength and its electronic energy is transferred to an acceptor represented as **A** that fluoresces at a longer wavelength [72,75].

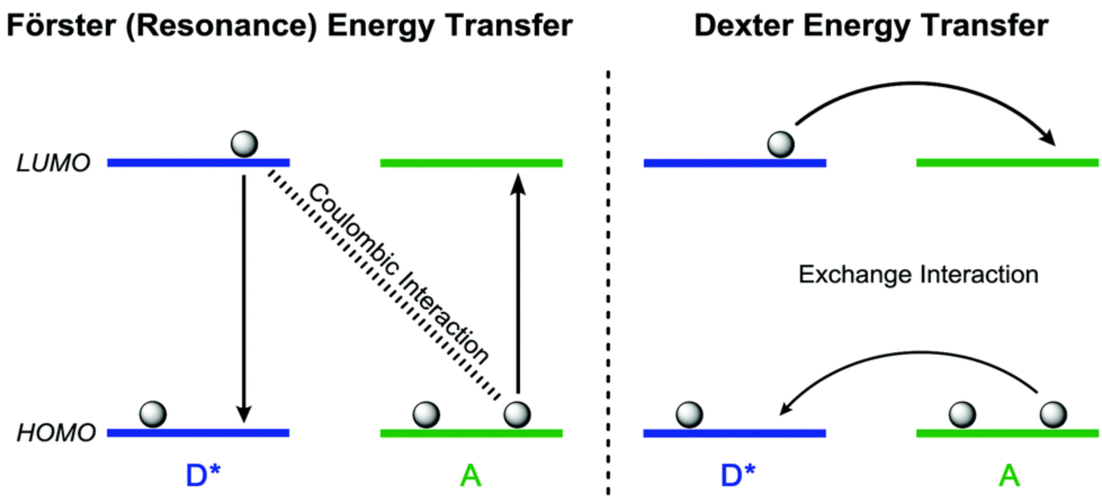

Figure 10: Energy transfer signal mechanisms through bond and spacer [75].

As previously mentioned, the most efficient energy transfer mechanism is determined by the distance between the acceptor receptor and donor units. Dexter electronic energy transfer mechanism is reported to occur at 10 Ǻ while the fluorescence resonance energy transfer system is greater than 10 Ǻ but less than 100 Ǻ [73–75].

1.3 Thesis Objectives

The aim of this study is to develop a polymeric-derived fluorescent sensor that can detect Fe (III) ions selectively in an acetic aqueous medium. Particularly to:

- combine the inherent fluorescent characteristics of urolithins with the biocompatibility nature of chitosan to develop a novel eco-friendly fluorescent probe.
- characterize the as-synthesized urolithin modified chitosan fluorescence chemosensor using various spectroscopic tools.
- investigate the selectivity of the as-synthesized fluorescence chemosensor Fe^{3+} ion in competitive metal ions environment.
- establish its performance and response under various environmental conditions.
- establish the nature of signaling sensing mechanism for the Fe^{3+} ion detection.

1.4 The Framework of the Thesis

Chapter 1: **Introduction**; provides general background knowledge regarding heavy metal pollution, common sensing platforms and introduces fluorescence-based chemosensors and prevailing signal mechanisms.

Chapter 2: **Literature Review**; overview of various fluorescence-based chemosensors for iron (III) detection, reported mechanisms and performances are discussed.

Chapter 3: **Methodology**; reagents and materials, research methods, spectroscopic and analytical characterizations used are discussed. Effects of influencing parameters on the performance of the as-synthesized urolithin modified chitosan fluorescence chemosensor are depicted.

Chapter 4: This section examines and interprets the findings, patterns, and observations.

Chapter 5: summary of results, observations and patterns are outlined, as well as guidelines for future studies.

Chapter 2

LITERATURE REVIEW

Several small organic compound-based sensors have been introduced in response to growing interest in fluorescence sensors over the last few decades. Despite their performance, these sensors have a number of disadvantages, including poor sensitivity in a multi-target media, a slow response time, higher solubility in organic solutions, limited pH range, and poor biocompatibility [25,38]. These flaws make it impossible for fluorescent small molecular probes to recognize metal ions selectively and sensitively.

By incorporating suitable receptor units into a functional polymer backbone, polymer-based probes have emerged as the most sought-after materials of the next decade, featuring enhanced aqueous solubility, structural stability, improved binding efficiency, enhanced signals, increased selectivity and biocompatibility [76–85].

2.1 Polymer-based Fluorescent Chemosensor

Polymers are high-molecular-weight synthetic or natural compounds made up of a number of repeating subunits. Because of their wide variety of properties, play an ubiquitous and important role in everyday life. Various polymers having fluorescence capabilities have been exploited for the production of optical probes with excellent performances [85–95]. Natural polymers, especially chitosan (shown in Figure 11) with deacetylated D-glucosamine unit linked with the N-acetylated unit is viable polysaccharide due to their unique physicochemical characteristics, biodegradability and good biocompatibility [83–87].

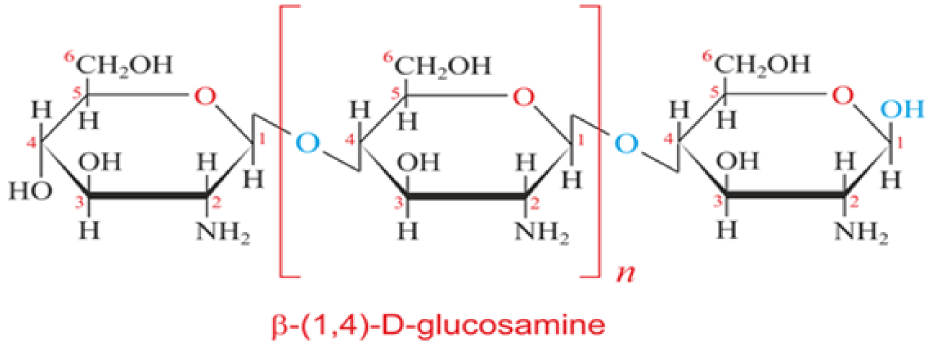

Figure 11: Structure of chitosan [87]

Chitosan's high hydroxyl and amino functional group content makes it suitable for covalent grafting reactions. It's worth noting that chitosan's low toxicity makes it a suitable material for a number of applications, including pollutant (like heavy metals) sequestering and detection, drug delivery, and optical devices [84,85].

For instance; Maityet al. [96] developed a fluorescent hydrogel based on chitosan that can exhibit dual mode; decreased fluorescence in when Fe^{2+} is present in the system and stronger and brighter fluorescence signals in the presence of Fe^{3+}. The lowest concentrations detected ranges within 0.124 and 0.138nM for Fe^{2+} and Fe^{3+}, respectively. Their findings shed light on the development of polymer-based fluorescent probes that are both biocompatible and degradable. The sensing mechanism is shown in Figure 12.

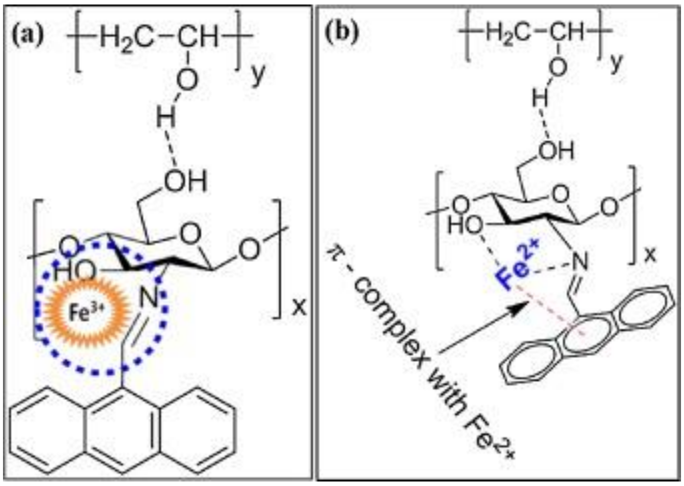

Figure 12: Chitosan-based fluorescent probe for Fe^{2+} and Fe^{3+} detection [96].

By a Schiff base reaction, a new fluorescent chitosan hydrogel was prepared by Fan et al. [97] in the presence of chitosan and terpyridinaldehyde monitoring for Fe^{2+} in aqueous media. They reported that the average detection limits ranges from 0.28 ppm to 3.8 ppm as shown in Figure 13. Xiong et al. [98] used an acylation reaction procedure to develop chitosan derivative probes that are sensitive and selective towards nitrophenol-based compounds in explosives; the authors reported 0.28μM as the lowest detection limit.

In the work of Xiong et al. [98], they synthesized a series of fluorescent chitosan derivatives probes by acylation reaction, which had a strong selectivity for 2,4,6-trinitrophenol and *p*-nitrophenol in explosives, high sensitivity, a low detection limit.

By grafting coumarin derivatives onto chitosan via Schiff base or acidified amine condensation reactions, Xiong et al. [99] developed a wide range of hydrogels based on chitosan for cation detection in diary wastewater. The authors reported a low detection limit of 9.6 μM; compared with the original chitosan, the grafted chitosan-based hydrogel probes demonstrated better fluorescence and sensing properties.

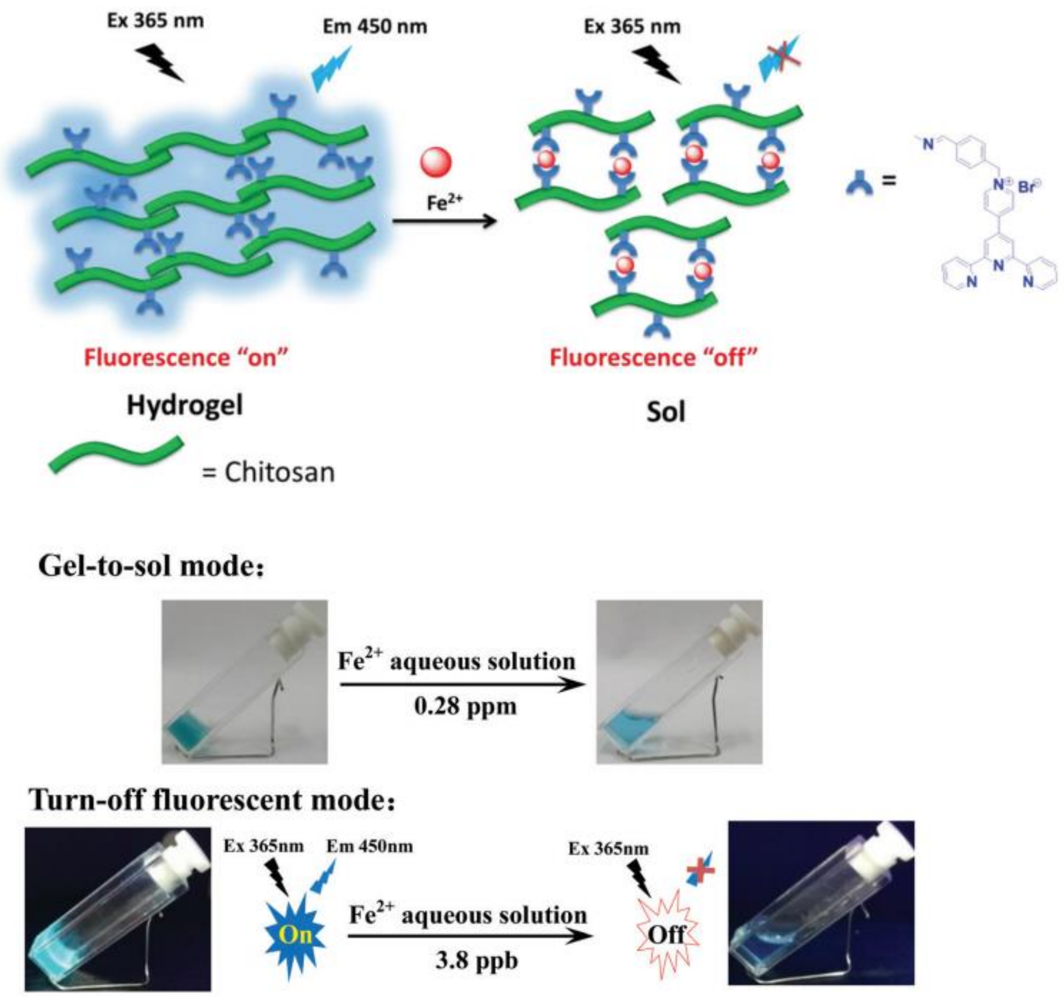

Figure 13: Fluorescence quenching phenomenon of chitosan-based hydrogel probe [97].

In 2012, Meng et al. [100] developed various chitosan-based probes with sufficiently high fluorescent potentials. One of the chitosan based probes was modified by fluorescein and the other by carbazole-based compound. These biocompatible probes demonstrated remarkable performances in serum and water samples during the detection of Fe^{3+} as shown in Figure 14. Particularly, at 516 nm and pH.7.2; the fluorescein modified chitosan quenched 94% bright green fluorescence in 100% water buffered TrisHCl solution. This performance was attributed to the paramagnetic nature of Fe3+ ion and the PET signal mechanism of the probe.

The authors reported a linear relationship with increases in the iron (III) concentration from 0 until 0.6 ppm in spinach juice while 0.4 ppm was recorded as the lowest limit of detection. However, at 508 nm, the carbazole modified probe quenched 60% of the observed green fluorescence.

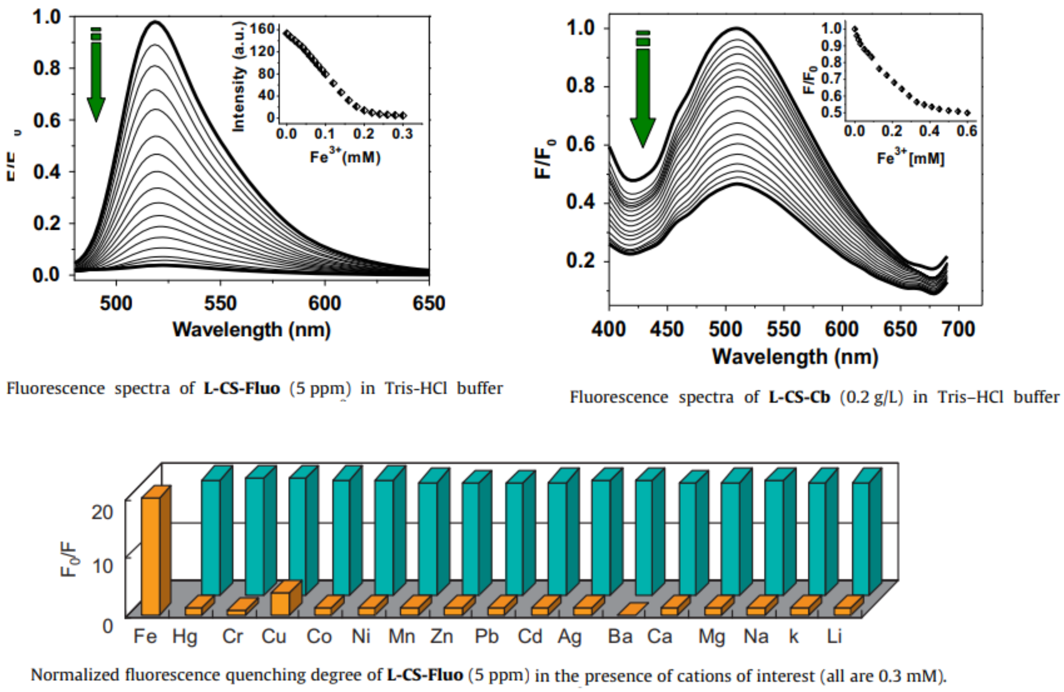

Figure 14: Sensing responses of fluorescent probes based on modified chitosan [100].

Also, conjugated polymers have been utilized as biocompatible fluorescent materials for metal ions detection attributed to their high sensitivity, remarkable selectivity and low cost [101]. Conjugated polymers typically consist of side chains having multifunctional groups on their backbones with various inherent fluorescent performances during target identification [101]. Since their side chains can be adjusted with different active compound or needed organic groups to further improve their sensing capabilities, conjugated polymers are especially appealing for the production of optical sensors.

Lee et al. [87] synthesized fluorescence biopolymer based on low-molecular-weight chitosan shown in Figure 15; the biopolymer-based fluorescence probe demonstrated excellent sensitivity and high selectivity during the detection of Cu^{2+} in the aqueous media, according to the researchers.

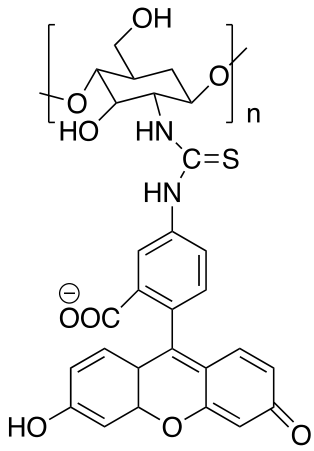

Figure 15: The molecular structure of chitosan-based fluorescence probe [87].

Ji et al. [104] developed a multi responsive polymer fluorescent probe based on dibenzo compound and a dibenzylammonium salt cross-linker for rapid sensing of K^+ ion. The conjugated polymeric fluorescent probe exhibited a weak fluorescence in 1% v/v $CHCl_3/CH_3CN$ solution as a result of polymer chain aggregation. The network of the polymeric chains collapsed after being treated with K^+, and the fluorescence was restored with a strong signal, as shown in Figure 16.

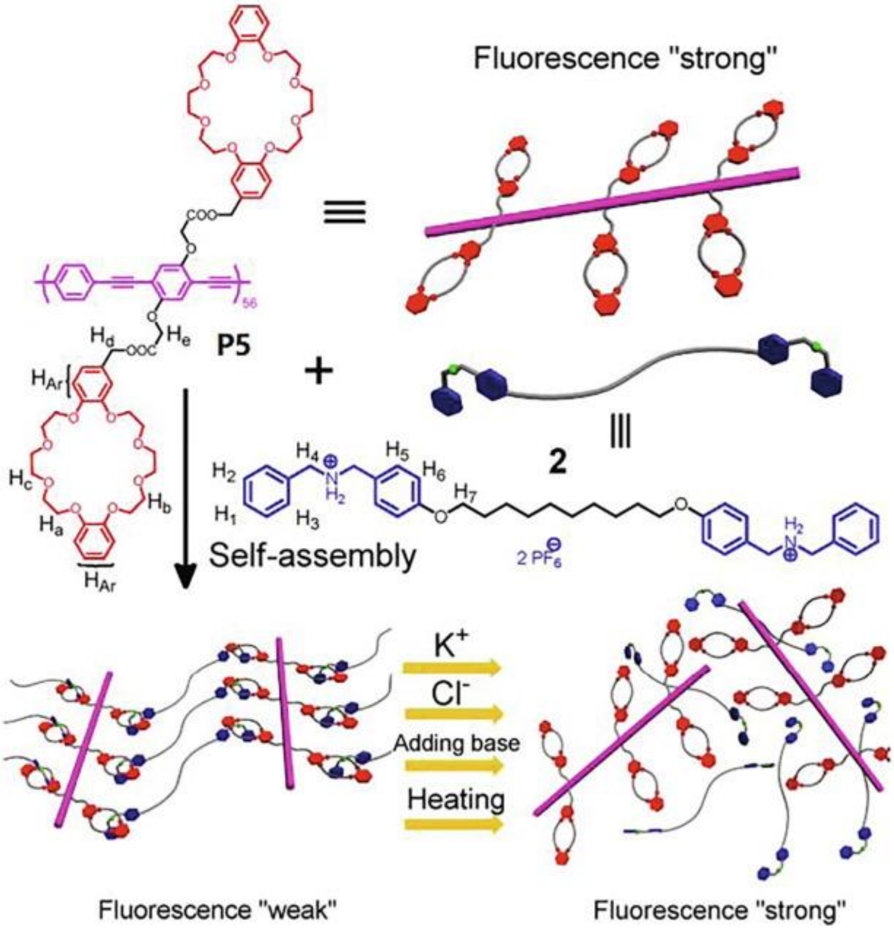

Figure 16: Fluorescence mechanism of conjugated polymer-based K^+ probe [104].

2.2 Urolithins

Urolithins are human microflora metabolites of derivatives of dietary ellagic acid, such as ellagitannin [105,106]. They are formed in the human gut and, after ingestion of ellagitannin-containing foods such as red raspberries, pomegranate, oak-age red wine, strawberries, walnuts or, they are present in the urine in the form of urolithin B glucuronide [105–107]. Urolithin A, B, C, and D are the four isomer forms of urolithin that have been described in the scientific literature [107].

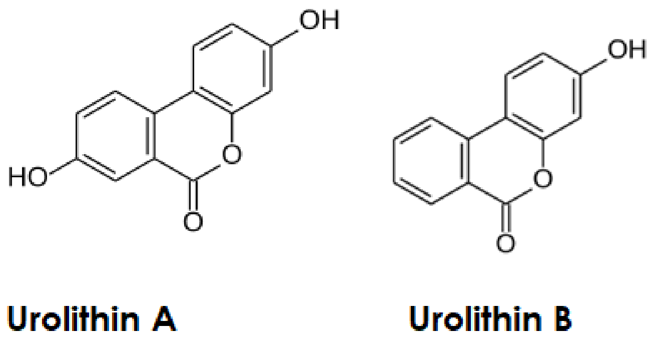

Figure 17: The structures of isoforms of Urolithins A and B.

Urolithin A is a metabolite compound that belongs to the class of organic compounds known as dibenzo-α-pyrones or benzo-coumarins and resulting from the transformation of ellagitannins by the gut bacteria. It is ubiquitous in edible plants, such as strawberries and pomegranates and has been the subject of preliminary studies due to its biological effects [105]. While urolithin B is a type of phenolic compounds produced in the human gut after absorption of ellagitannins-containing food [105,106].

Previous research has shown that urolithins have a large Stoke shift and a high quantum yield with no drastic overlap between the spectra [108]. Urolithins are also simple to synthesize and modify, have a long spectral wavelength, and are non-toxic [107-109]. From this viewpoint, this research was directed to combine the inherent fluorescent characteristics of urolithins with the biocompatibility nature of chitosan to develop a novel eco-friendly fluorescent probe.

2.3 Iron (III) Ion Detection by Fluorescent Chemosensor

Iron ions are commonly found in the human body and representing the largest among the transition metals, with an average content of 5% in the soil [99, 100]. Although iron is a critical element, excessive intake poisons various body organs [82,84]. For the selective detection of Fe^{3+}, several technologies have been reported. Among these technologies is fluorescent probes commonly applied due to their low cost, selectivity, sensitivity and rapid response. Meng et al. [100] synthesised various chitosan modified fluorescence dye probes according to the schematic pathways shown in Figure 18.

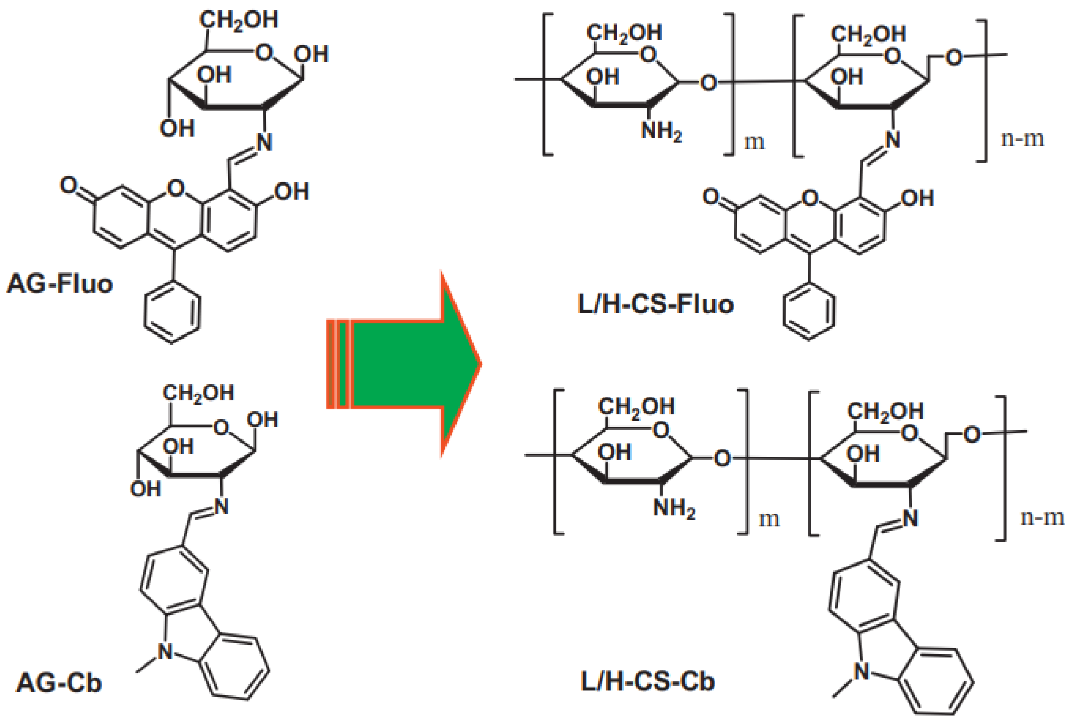

Figure 18: Synthesis of chitosan-based fluorescent probes for Fe^{3+} detection [100].

The fluorescence strength of the as-synthesised materials easily attained equilibrium with the addition of Fe^{3+}, and quenched 60–97% of the fluorescence. The probe developed a 1:1 complex with the target cation in the system, according to the authors, with an interaction constant of 2.20×10^{6} M^{-1} and 0.2 ppm was obtained as the limit of detection. In the presence of both monovalent and divalent metal ions, the authors found no major changes in the intensities of the fluorescence. While the addition of Cu^{2+} and Hg^{2+} ions to the suspensions did not quench the fluorescence significantly, the Fe^{3+} ions addition resulted in a severe quenching of the intensity of the fluorescence, confirming that the AG-Fluo probe had the highest Fe^{3+} binding affinity.

Although they recorded a mild fluorescence quenching after the addition of Hg^{2+} and Cu^{2+}; the addition of Fe^{3+} ions to the suspensions resulted in the drastic quenching of their fluorescence intensities, confirming that the AG-Fluo probe had the strongest binding affinity to Fe^{3+}.

In 2016, Li and co-workers [51] developed L-cysteine capped Fe_3O_4@ZnO for detection of Fe^{3+}. According to the authors, the binding of Fe^{3+} to the as-synthesized probe induced an apparent decrease of the fluorescence which was enhanced by the magnetism of the probe enables which effectively decreased the interference within the matrix. The synthesis route and the binding mechanism is shown in Figure 19; in both wastewater and serum samples, they found a detection limit of 3 nmol L^{-1} and a fast response time lower than 1 minute.

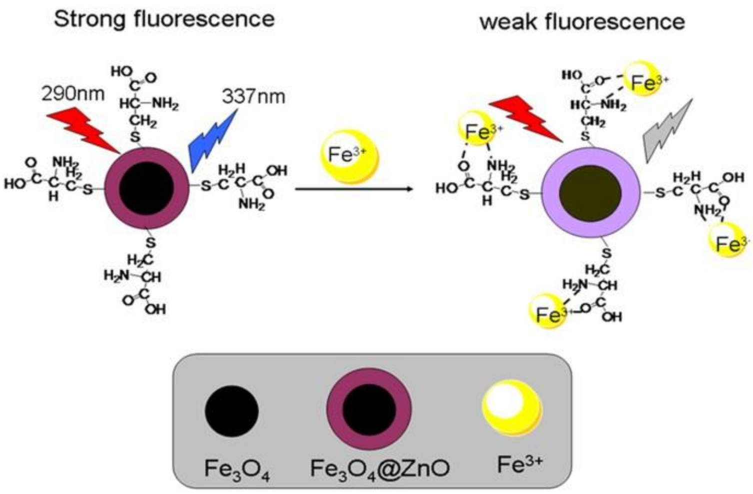

Figure 19: Fe^{3+} detection mechanism by iron oxide based probe [51].

Sheng et al. [110] developed a fluorescent probe which was based on rhodamine material with excellent Fe^{3+} selectivity in the mixture containing Cr^{3+}. Notably, the probe is water-soluble and the enhanced selectivity was achieved, according to the scientists, by adding another coordination moiety to the precursor's chelating moiety.

According to the researchers, adding equal Fe^{3+} ions to the probe solution in an aqueous buffer caused a vivid fluorescence emission with a strong color change to red from colourless. The addition of Mg^{2+}, Ca^{2+} and K^+ had only a slight effect on the spectra response of the as-synthesised probe, even at concentrations which is nearly 40 times that of the Fe^{3+}. Other competitive cations shown in Figure 20 did not cause a noticeable change in probe fluorescence, according to the data.

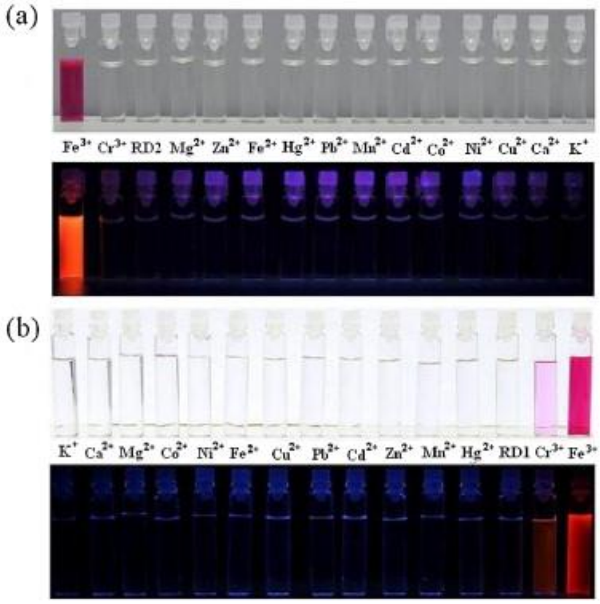

Figure 20: Fe^{3+} probe showing color variation under hand-held ultraviolet and normal light lamps [110].

In the year 2020, Fallah et al. [111] produced a urolithin-based fluorescent probe for the selective detection of Iron (III) in 1% v/v DMSO/H2O. The selectivity of the iron (III) sensing probe is independent of the presence of other tested metals, according to the authors. Furthermore, the authors concluded that the lactone group was responsible for the interaction with iron (III), as seen in Figure 21, since hydroxyl and/or methoxy substituents on the probe did not result in a change in stoichiometry as determined by Job's plots.

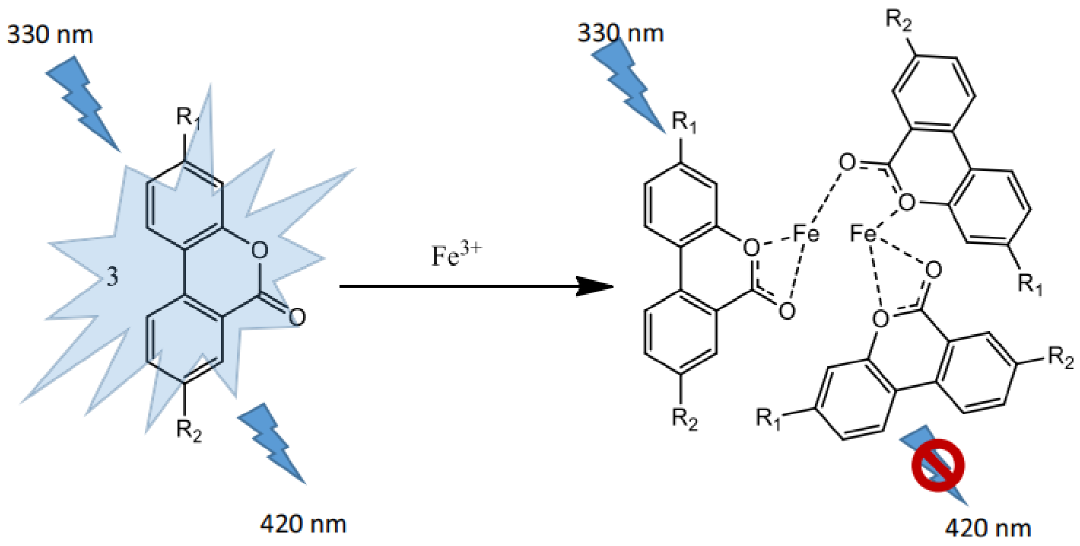

Figure 21: The mechanism of the urolithin-based probe for Fe^{3+} detection [111].

Zhang et al. [112] synthesized a fluorescent sensor which is based on a dual-response mode by using quinoline modified compound as the fluorophore for the rapid assessment of iron (III) and copper (II) ions in various aqueous solutions. At pH 7.2 in 50 mM Tris buffer; the fluorescent sensor demonstrated a desirable selectivity. According to the researcher, the as-synthesized probe had no noticeable interference in the multi-cation environment while it remarkably recognized Cu^{2+} and Fe^{3+} as illustrated in Figure 22.

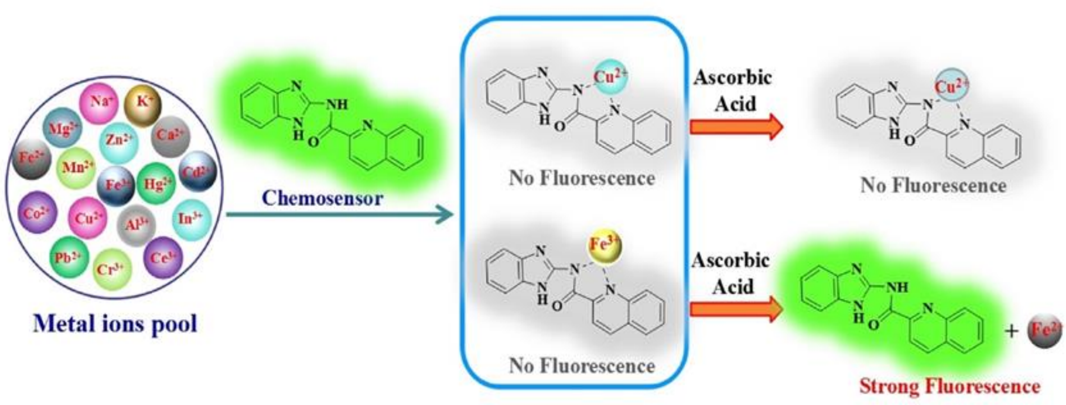

Figure 22: Illustration of the detection for Cu^{2+} and Fe^{3+} by a fluorescent probe [122].

Madhu and Sivakumar [113] synthesized a pyridine-based “turn-off” fluorescent probe for on site detection and monitoring of Fe^{3+} in a mixture containing varying concentration of cations 9:1 v/v DMSO/H_2O solution. They obtained a binding constant of $5.1–6.1 \times 10^{-2}$ M from both the UV–vis and fluorescence spectral responses with a 5 –88 nM detection limits; their study is represented in Figure 23.

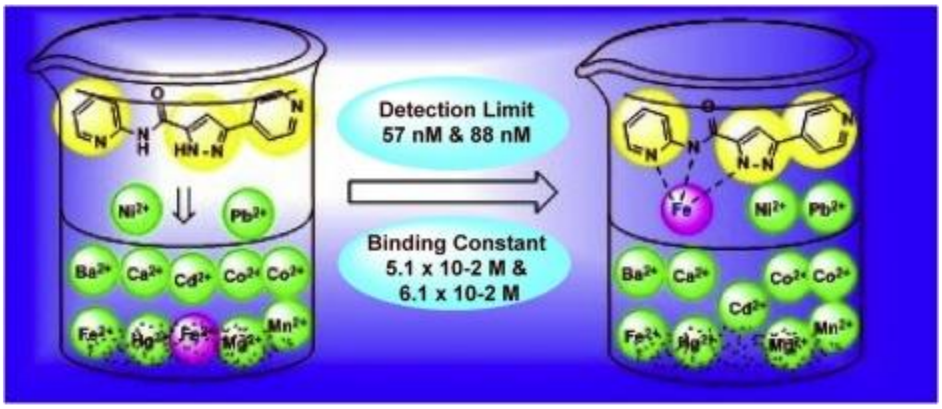

Figure 23: Illustration of the detection of Fe^{3+} by “turn-off” fluorescent probe [113].

Chapter 3

EXPERIMENTAL

3.1 Reagents and Materials

Distilled water was used during the preparation of the metal ion stock solutions and all the reagents were of analytical grade and were not purified before use. All the chemicals were purchased from Merck KGaA and Sigma-Aldrich Co., Germany. Here is list of the materials used: 1-bromo-3-chloroprene, chitosan, resorcinol, sodium chloride, mercury (II) chloride, sodium hydroxide, acetone, 1,4-dioxane, cobalt (II) nitrate hexahydrate, silver nitrate, nickel (II) nitrate hexahydrate, barium sulfate, acetic acid, zinc sulfate heptahydrate, boric acid, aluminium sulfate, sodium hydride, potassium chloride, 2-iodobenzoic acid and iron (III) nitrate nonahydrate. The stock solution of metal ions was prepared with distilled water.

3.2 Instruments: Infrared spectra and Chromatography

To evaluate the functional groups on the synthesised samples, a Fourier transform infrared FTIR-8700 spectrophotometer (Shimadzu FR-IR Prestige 21, Japan) was used in the range of 4000–400 cm^{-1}. Each study used 30 mg of dried powder sample without the use of a KBr disc. Thin-layer chromatography (TLC) was used to evaluate the reaction's progress by determining the R_f value at each point. Silica gel plates-containing aluminium were used for the TLC.

After adding metal ions to a 1 percent v/v acetic acid solution, the fluorescence spectra were obtained using a 96-well microplate reader with a 330 nm excitation wavelength and a 500 nm/min scan rate. Particularly, to prepare the stock solution of the probe, known amounts of the as-prepared Uro-*m*-Ch were dissolved in 100 mL 1% v/v acetic acid/H_2O. A 165 μL of 0.15 percent per metal ion solution (i.e. B^{3+}, Na^{+}, Ni^{2+}, Zn^{2+}, Fe^{3+}, Ag^{+}, Ba^{2+}, Co^{+}, Al^{3+}, Hg^{2+}, K^{+}) in 1 percent acetic acid solution was applied to the 165 μL of 0.15 percent stock solution of the Uro-*m*-Ch and thoroughly mixed; afterwards, the fluorescence measurement was performed.

3.3 Method

3.3.1 Synthesis of 3-hydroxy-6H-benzo[c]chromen-6-one (Uro-B)

Uro-B was synthesized using a modified version of a previous technique [108,111]. In a nutshell, 10 grams of resorcinol is dissolved in 4.4 grams of sodium hydroxide and 60 milliliters of distilled water. The reaction flask was then filled with 7.5 g of 2-iodobenzoic acid. For 1 hour, the mixture was refluxed. Following that, 10 mL of copper sulphate solution (25%) was applied dropwise. The solution mixture was precipitated, filtered, and washed with ice-cold water, yielding a 90 percent product; Figure 24 depicts the synthesis pathway.

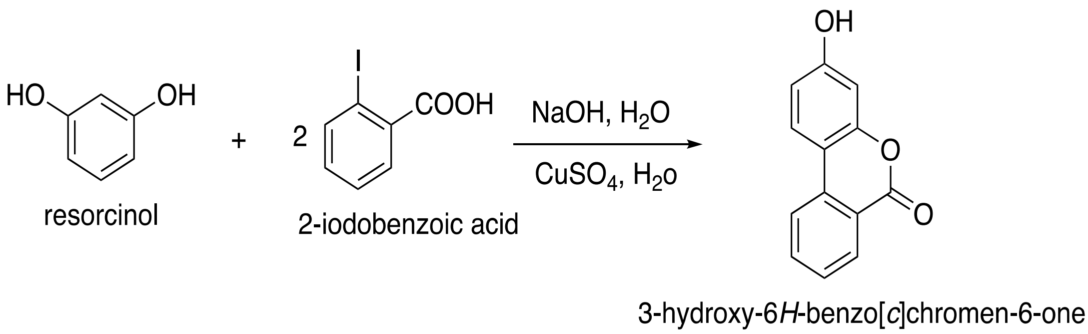

Figure 24: The synthesis pathway for Uro-B.

3.3.2 Synthesis of 3-(3-chloropropoxy)-6H-benzo[c]chromen-6-one (Uro-Cl)

The Uro-Cl was prepared according to the procedure described herein: To a solution of 3 g Uro-B in 40 mL DMF, 1.5 g sodium hydride was added. At room temperature, the solution was stirred for 5 minutes before adding 10 g of 1-bromo-3-chloropropane to the reaction mixture. The mixture was stirred for 1 hour before being poured into a 50 mL 0.1 N aqueous NaOH solution and filtered then washed with n-hexane solution; the synthesis shown in Figure 25 yielded 85 percent of final product.

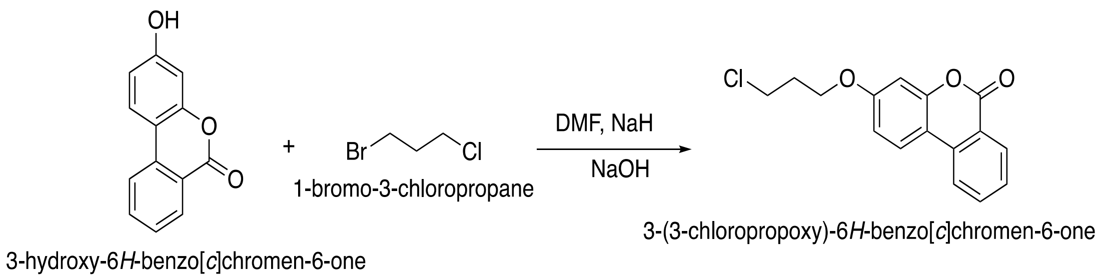

Figure 25: The synthesis pathway for Uro-Cl.

3.3.3 Preparation of Uro-*m*-Ch

The procedure for the synthesis of Uro-*m*-Ch is described here as follows. In 30 mL of 2% acetic acid solution, 0.2 g chitosan was dissolved and vigorously stirred until a uniform viscous solution was obtained. The chitosan solution was then treated with 50 mg of Uro-Cl in 20 mL 1,4-dioxane. At 30°C, the mixture was refluxed for 12 hours. Finally, to the chitosan mixture above, acetone and 200 mL 1,4-dioxane solution (3:4 v/v) was added, stirred, and the obtained precipitate was filtered then repeatedly washed with acetone. The entire synthesis routes from Uro-B to Uro-*m*-Ch is illustrated in Figure 26.

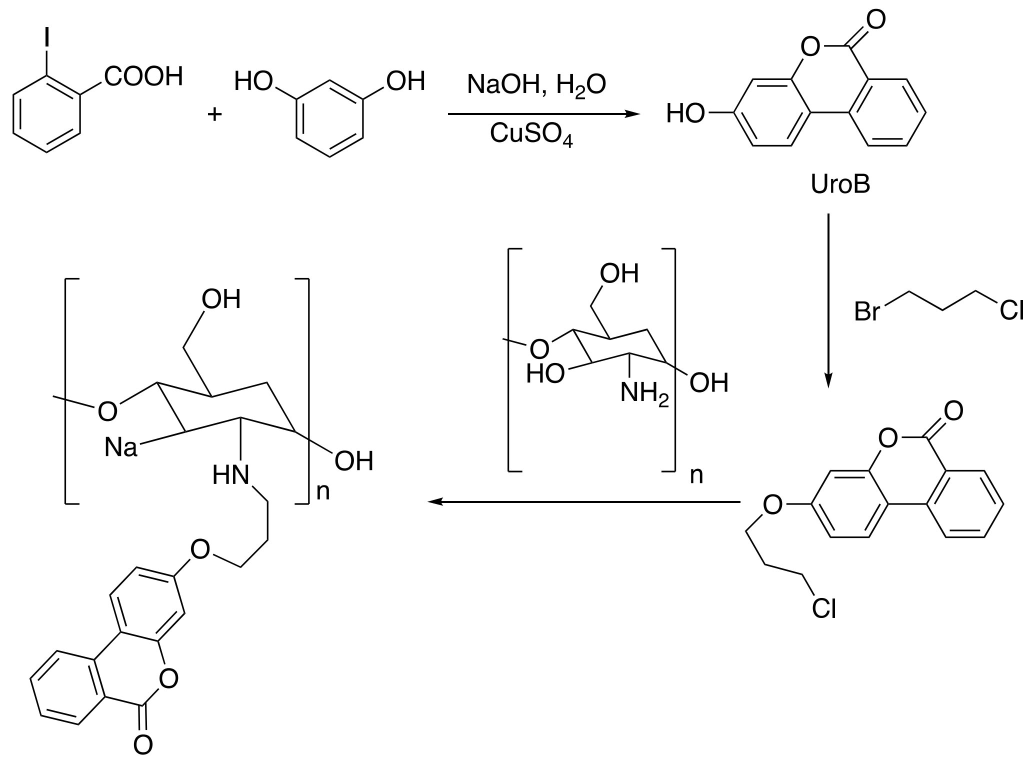

Figure 26: Illustration of the routes for the synthesis of urolithin modified chitosan probe

Chapter 4

RESULTS AND DISCUSSIONS

4.1 Characterization

4.1.1 FTIR Spectra of Starting Material, Precursor and Modified Product

The FTIR spectra obtained after the synthesis was employed to establish the presence of functional groups in each sample and to ratify the successful synthesis of the urolithin-based chitosan; Figure 27 depicts the obtained spectra.

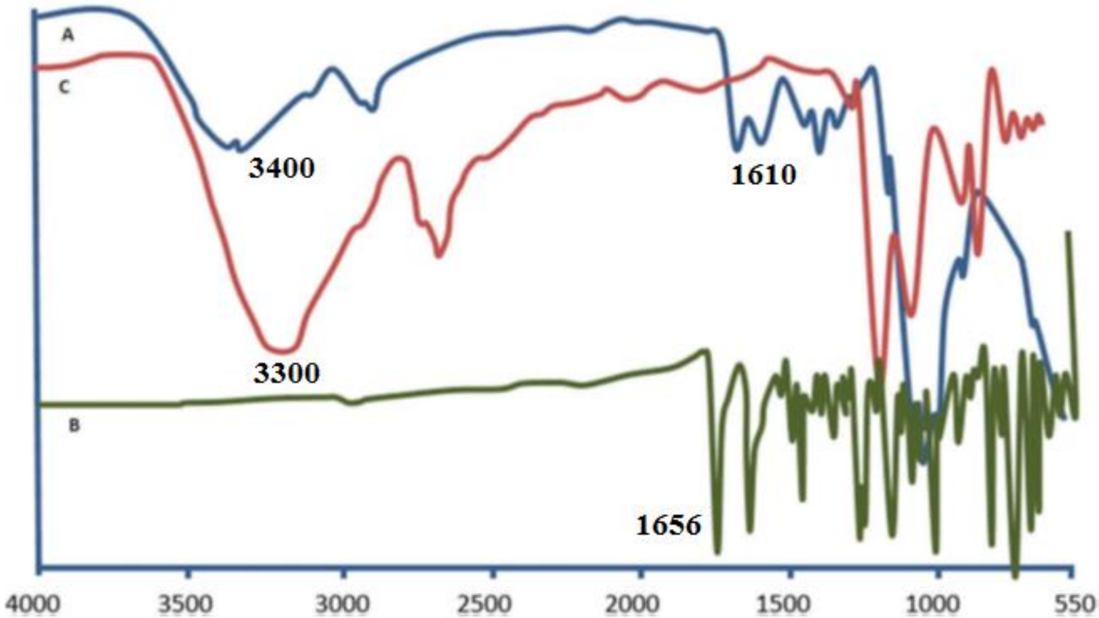

Figure 27: The FTIR spectra of the precursors and final products (A: chitosan; B: Uro-Cl and C:Uro-*m*-Ch).

According to the spectrum of chitosan depicted in Figure 27(A); the bands detected around 3500−3300 cm^{-1} are attributed to hydroxyl and N–H groups while the characteristics chitosan peaks were observed at 1656 cm^{-1} and 1587 cm^{-1} which are associated with amide I and N–H deformation, respectively. The peaks at 566, 756, 1179 and 2873 cm^{-1} represent bending NH, C–O bending; stretching of C–O–C and the stretching of C–H stretching, respectively. These peaks are consistent with several other reports. There is no vibration was observed considering the Uro-Cl spectrum from 3500 to 2000 cm^{-1} while sharp peaks are observed from 1700 to 550 cm^{-1}. Notably, the lactone carbonyl stretching appeared at 1727 cm^{-1} while at 1656 cm^{-1} the C=O deformation was obtained. As expected, the urolithin modified chitosan sample featured peaks from chitosan and Uro-Cl with both reduced and intensified bands. Particularly; the characteristics chitosan peaks disappeared after the modifying while the carbonyl stretching shifted to a lower wavelength. The reduced intensity in the peaks of the Uro-*m*-Ch spectrum is likely due to the interaction between the C=O of urolithin and the OH/amine groups of chitosan via a hydrogen bonding mechanism.

4.1.2 Characterization of the Uro-*m*-Ch by Fluorometric Measurement

According to the previous reports by Fallah et al [108,111], urolithin B (Uro-B) exhibited fluorometric characteristics. However, considering the fact that chitosan lacks fluorescence potential naturally; the fluorometric capacity of the as-synthesised Uro-*m*-Ch was investigated. Following the previously reported procedures [111]; the optical characteristics of the as-synthesized urolithin-based chitosan probe in 1% v/v of CH_3COOH/H_2O was investigated and shown in Figure 28.

As shown in Figure 28, the maximum excitation wavelength was obtained which hovers from 290 nm to 330 nm while 430 nm is the maximum emission spectrum when excited at 330 nm. A large Stokes shift of 100 nm demonstrated the fluorescence capability of the synthesised sample.

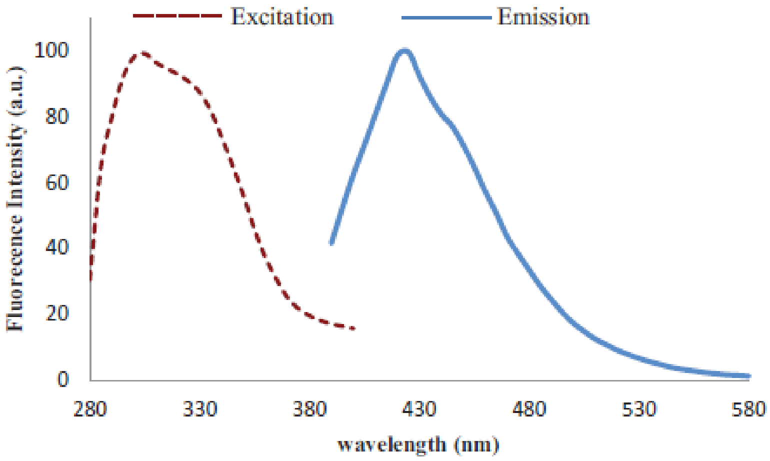

Figure 28: The optical spectra of Uro-*m*-Ch.

4.1.3 Performance of Uro-*m*-Ch in various Fe^{3+} ion Concentrations

The fluorescence responses of the as-synthesized urolithin-based chitosan probe with respect to different iron (III) concentrations (0.10–0.080 mM) were examined in 1% v/v CH_3COOH/H_2O solution. The spectra responses of the Uro-*m*-Ch probe are tabulated and depicted in Table 1 while corresponding data are plotted and shown in Figure 29. As seen, Uro-*m*-Ch exhibited the λ_{max} emission at 420 nm. With increases in the iron (III) concentration, a proportional decreasing trend in fluorescence intensity was observed, which reached a nearly non-fluorescence point. Figure 29 inset shows that the emission intensity and the variation in concentration of iron (III) is nearly associated, demonstrating a statistically significant fluorescence quenching nature of Uro-*m*-Ch.

Table 1: Uro-*m*-Ch fluorescence responses with respect to increasing Fe^{3+} concentration

Iron (III) ion concentration mM	F	F_0	F/F_0
0.0002	75	100	0.70
0.0003	70	100	0.75
0.0004	58	100	0.58
0.0005	45	100	0.45
0.0006	33	100	0.33
0.0007	23	100	0.23
0.0008	20	100	0.20
0.0009	17	100	0.17
0.001	7	100	0.07

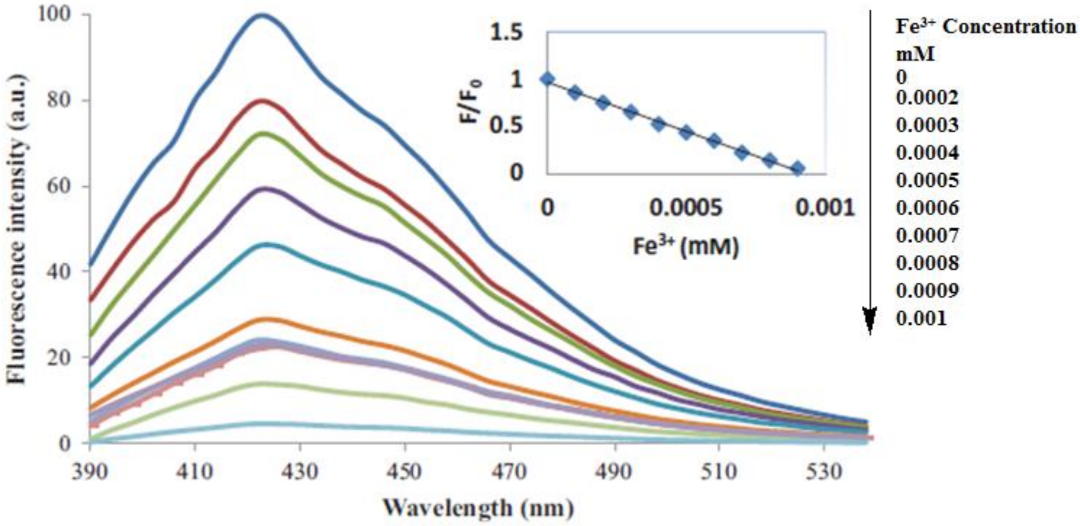

Figure 29: Response of Uro-*m*-Ch with respect to variation in Fe^{3+} concentration.

The interaction of iron (III) ion with the lactone group of urolithin or the hydroxyl moiety of the chitosan backbone could cause Uro-*m*-Ch fluorescence quenching through electron or intramolecular energy transfer. No overlap was observed between the absorption and emission spectra; as a consequence, the energy and/or electron transfer from the Fe^{3+} ion to the excited state of the Uro-*m*-Ch could result in non-radiative decay, as previously stated. [108,111].

4.1.4 Selective Responses of Uro-*m*-Ch in the Presence of Metal Ions

In the presence of mono and multivalent cations (i.e. Co^{2+}, Ag^{+}, Al^{3+}, Zn^{2+}, Ba^{2+}, Hg^{2+}, K^{+}, Na^{+}, B^{3+}, Ni^{2+}), the selectivity of Uro-*m*-Ch as an effective probe against Fe^{3+} ion was investigated. As a result, 165 µL of 0.15 percent per metal ion solution in 1 percent acetic acid was applied to 165 µL of 0.15 percent Uro-*m*-Ch solution. Obtained responses of Uro-*m*-Ch under the selectivity studies are shown in Table 2 and corresponding data plotted in Figure 30. From the results shown in Figure 30; Uro-*m*-Ch demonstrated a remarkable quenching effect only with Fe^{3+} ion. Uro-*m*-Ch was discovered to be a selective probe for iron (III) under the same experimental procedures, as no quenching was observed with the interfering cations.

Table 2: Uro-*m*-Ch responses in the presence of interfering cation ions

Cations	F	F_0	F_0/F
Na^{+}	525	630	1.20
Ag^{+}	623	630	1.01
K^{+}	588	630	1.07
Co^{+}	577	630	1.09
Fe^{3+}	95	630	6.63
Ni^{2+}	574	630	1.09
Ba^{2+}	591	630	1.06
Zn^{2+}	593	630	1.06
Hg^{2+}	570	630	1.10
Al^{3+}	579	630	1.08
B^{3+}	576	630	1.09

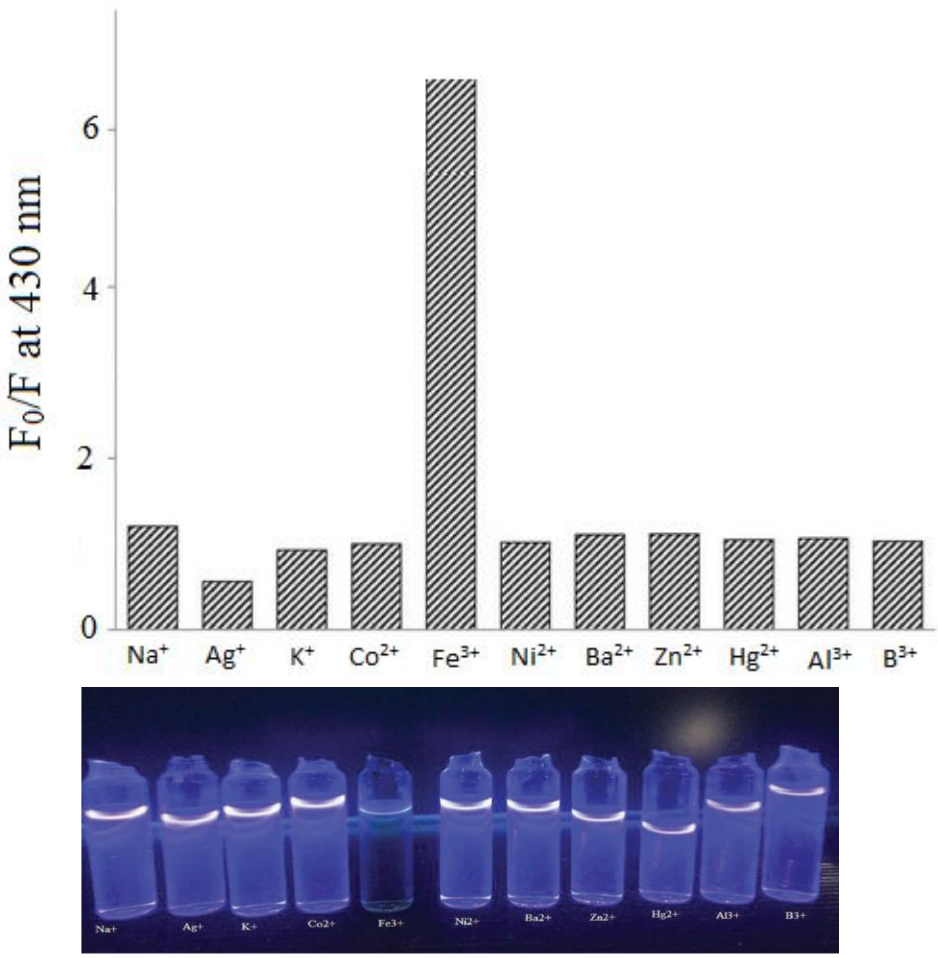

Figure 30: Selectivity of Uro-*m*-Ch probe in various cations matrices

4.1.5 Interference Study

Interference study of Uro-*m*-Ch for 0.1 mM Fe^{3+} ion was further examined in the presence of 0.5 mM various metal ions in 1% (v/v) CH_3COOH/H_2O; then compared with the probe without the interference. The results obtained are depicted in Table 3 and Figure 31; note that the Uro-*m*-Ch probe without interference maintained stable fluorescence quenching effects on Fe^{3+} ion, While the anti-interference analysis showed that other cations have no effect on the interaction between the probe and the iron (III).

This observation is consistent with the study of Fallah et al [111] who established the anti-interference performances of the Urolithin A and B derivatives for iron (III) detection.

Table 3: Fluorescence intensity of Uro-*m*-Ch under the interference study.

Probe composition	**Intensity**
Uro-*m*-Ch	630
Uro-*m*-Ch + Na^+ mix with Iron (III)	97
Uro-*m*-Ch + K^+ mix with Iron (III)	100
Uro-*m*-Ch + Co^+ mix with Iron (III)	95
Uro-*m*-Ch + Ag^+ mix with Iron (III)	98
Uro-*m*-Ch + Iron (III)	99
Uro-*m*-Ch + Ni^{2+} mix with Iron (III)	98
Uro-*m*-Ch + Ba^{2+} mix with Iron (III)	99
Uro-*m*-Ch + Zn^{2+} mix with Iron (III)	97
Uro-*m*-Ch + Hg^{2+} mix with Iron (III)	96
Uro-*m*-Ch + Al^{3+} mix with Iron (III)	97
Uro-*m*-Ch + B^{3+} mix with Iron (III)	97

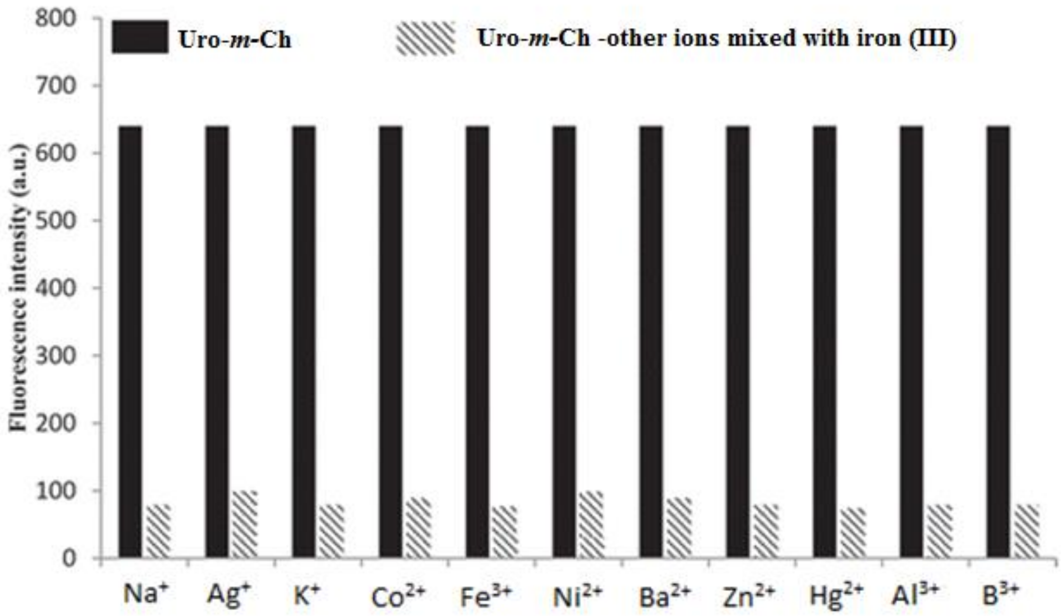

Figure 31: In 1% (v/v) acetic solution, the fluorescence response of the Uro-*m*-Ch probe to 0.1 mM Fe(III) in the presence of interfering cations.

A slight fluorescence quenching was observed after the addition of Ag^{+}, Ni^{2+} and Ba^{2+}, as shown in Figure 31. The introduction of the target iron ions to the suspensions, on the other hand, resulted in a dramatic decrease in fluorescence strength, suggesting that the Uro-*m*-Ch probe had the highest Fe^{3+} binding affinity. The addition of chitosan to the urolithin allowed membrane penetration and biocompatibility of the Uro-*m*-Ch probe, according to the findings.

Chapter 5

CONCLUSION AND FUTURE WORK

The goal of this PhD study was to build an environmentally friendly polymer-based fluorescence optical sensor that could detect iron (III) in acetic aqueous solution quickly and selectively. Firstly, a chitosan modified urolithin (Uro-*m*-Ch) probe was synthesized via a facile three steps synthesis routes, which resulted in ~85% yield. Obtained Uro-*m*-Ch sample was characterized; the FTIR results confirmed the presence of characteristics chitosan peaks and the C=O of the lactone group of the urolithin. Also, Uro-*m*-Ch demonstrated fluorescence character in the presence of 1% (v/v) CH_3COOH/H_2O solution.

The significant results obtained during the Uro-*m*-Ch sensing application under various conditions are summarized herein:

- In 1% v/v CH_3COOH/H_2O solution; Uro-*m*-Ch exhibited a maximum excitation wavelength (λ_{max}) within 290–330 nm and λ_{max} emission spectrum at 430 nm with Stokes shift of 100 nm without the target metal ion.
- In the presence of different iron (III) concentrations; Uro-*m*-Ch exhibited the λ_{max} emission at 420 nm in 1% v/v CH_3COOH/H_2O solution.
- With increases in the iron (III) concentration from 0.10 to 0.080 mM, a proportional decreasing trend in fluorescence intensity was observed which demonstrated the fluorescence quenching nature of Uro-*m*-Ch.

- In the presence of 0.1 mM interfering metal ions, Uro-*m*-Ch demonstrated a remarkable quenching effect only with Fe^{3+} ion.
- The fluorescence character of Uro-*m*-Ch towards Fe^{3+} ion was attributed to intramolecular energy/electron transfer due to the interaction of iron (III) ion with the lactone group of the urolithin and/or the hydroxyl moiety of the chitosan backbone.

In Future Work;

The as-synthesized Uro-*m*-Ch probe successfully demonstrated rapid and selective responses towards synthetic solutions containing the target iron (III) ion. However, further studies are needed to establish its industrial and field applications, including:

- An extension of the investigations of the performance of the Uro-*m*-Ch probe to real industrial, agricultural and municipal water is required in the presence of other anions and emerging interference.
- Variation in the concentration of the interference will be required to understand the response of the Uro-*m*-Ch probe in real and spiked water.
- The actual contribution of chitosan in the probe, its mechanism and comparative performances with other natural fluorescent polymers need to be established.

REFERENCES

[1] Masindi V., & Muedi K.L. (2018). Environmental Contamination by Heavy Metals, Heavy Metals, In: Hosam El-Din M et al. *IntechOpen*, DOI: 10.5772/intechopen.76082.

[2] von der Heyden, B.P., Roychoudhury, A.N. (2015). Application, Chemical Interaction and Fate of Iron Minerals in Polluted Sediment and Soils. *Curr Pollution Rep* 1, 265–279.

[3] Abbaspour, N., Hurrell, R., & Kelishadi, R. (2014). Review on iron and its importance for human health. *Journal of research in medical sciences: the official journal of Isfahan University of Medical Sciences*, *19*(2), 164.

[4] Harigae, H. (2018). Iron metabolism and related diseases: an overview. *International journal of hematology*, *107.*

[5] VanderMeulen, H., & Sholzberg, M. (2018). Iron deficiency and anemia in patients with inherited bleeding disorders. *Transfusion and Apheresis Science*, *57*(6), 735-738.

[6] Li, J., Wang, Q., Guo, Z. *et al.* (2016). Highly selective fluorescent chemosensor for detection of Fe^{3+} based on Fe_3O_4@ZnO. *Sci Rep* 6, 23558.

[7] Bojinov, V., & Georgiev, N. (2011). Molecular sensors and molecular logic gates. *Journal of the University of Chemical Technology & Metallurgy*, *46*(1).

[8] Beer, P. D., Gale, P. A., & Chen, Z. (1999). Electrochemical recognition of charged and neutral guest species by redox-active receptor molecules. In *Advances in Physical Organic Chemistry* (Vol. 31, pp. 1-90). Academic Press.

[8] Gai, L., Mack, J., Lu, H., Nyokong, T., Li, Z., Kobayashi, N., & Shen, Z. (2015). Organosilicon compounds as fluorescent chemosensors for fluoride anion recognition. *Coordination Chemistry Reviews*, 285, 24-51.

[9] Kumar, N., Bhalla, V., & Kumar, M. (2013). Recent developments of fluorescent probes for the detection of gasotransmitters (NO, CO and H2S). *Coordination Chemistry Reviews*, 257(15-16), 2335-2347.

[10] Kim, H. N., Ren, W. X., Kim, J. S., & Yoon, J. (2012). Fluorescent and colorimetric sensors for detection of lead, cadmium, and mercury ions. *Chemical Society Reviews*, 41(8), 3210-3244.

[11] Zhang, J. F., Zhou, Y., Yoon, J., & Kim, J. S. (2011). Recent progress in fluorescent and colorimetric chemosensors for detection of precious metal ions (silver, gold and platinum ions). *Chemical Society Reviews*, 40(7), 3416-3429.

[12] Goldhaber, S.B. (2003). Trace element risk assessment: Essentiality vs. toxicity. Regul. *Toxicol. Pharmacol*. 38, 232–242.

[13] Bansod, B., Kumar, T., Thakur, R., Rana, S. & Singh, I. (2017). A review on various electrochemical techniques for heavy metal ions detection with different sensing platforms. *Biosens. Bioelectron*. 94, 443–455.

[14] Farzin, L., Shamsipur, M., Sheibani, S..A (2017). review: Aptamer-based analytical strategies using the nanomaterials for environmental and human monitoring of toxic heavy metals. *Talanta* 174, 619–627.

[15] Manjare, S. T., Kim, Y., & Churchill, D. G. (2014). Selenium-and tellurium-containing fluorescent molecular probes for the detection of biologically important analytes. *Accounts of chemical research*, 47(10), 2985-2998.

[16] Longstreet, A. R., Jo, M., Chandler, R. R., Hanson, K., Zhan, N., Hrudka, J. J., ... & McQuade, D. T. (2014). Ylidenemalononitrile enamines as fluorescent "turn-on" indicators for primary amines. *Journal of the American Chemical Society*, 136(44), 15493-15496.

[17] Duke, R. M., Veale, E. B., Pfeffer, F. M., Kruger, P. E., & Gunnlaugsson, T. (2010). Colorimetric and fluorescent anion sensors: an overview of recent developments in the use of 1, 8-naphthalimide-based chemosensors. *Chemical society reviews*, 39(10), 3936-3953.

[18] Santos-Figueroa, L. E., Moragues, M. E., Climent, E., Agostini, A., Martínez-Máñez, R., & Sancenón, F. (2013). Chromogenic and fluorogenic chemosensors and reagents for anions. A comprehensive review of the years 2010–2011. *Chemical society reviews*, 42(8), 3489-3613.

[19] Chen, X., Zhou, Y., Peng, X., & Yoon, J. (2010). Fluorescent and colorimetric probes for detection of thiols. *Chemical Society Reviews*, 39(6), 2120-2135.

[20] Jung, H. S., Chen, X., Kim, J. S., & Yoon, J. (2013). Recent progress in luminescent and colorimetric chemosensors for detection of thiols. *Chemical Society Reviews*, 42(14), 6019-6031.

[21] Zhou, X., Lee, S., Xu, Z., & Yoon, J. (2015). Recent progress on the development of chemosensors for gases. *Chemical reviews*, 115(15), 7944-8000.

[22] Salinas, Y., Martínez-Máñez, R., Marcos, M. D., Sancenón, F., Costero, A. M., Parra, M., & Gil, S. (2012). Optical chemosensors and reagents to detect explosives. *Chemical Society Reviews*, 41(3), 1261-1296.

[23] Wang, B., & Anslyn, E. V. (Eds.). (2011). *Chemosensors: principles, strategies, and applications* (Vol. 15). John Wiley & Sons.

[24] Demchenko, A. P. (2009). Fluorescence detection techniques. *Introduction to fluorescence sensing*, 65-118.

[25] Gao, X., Li, X., Li, L., Zhou, J., & Ma, H. (2015). A simple fluorescent off–on probe for the discrimination of cysteine from glutathione. *Chemical Communications*, 51(45), 9388-9390.

[26] Cardona, M. A., & Magri, D. C. (2014). Synthesis and spectrophotometric studies of water-soluble amino [bis (ethanesulfonate)] azobenzene pH indicators. *Tetrahedron Letters*, 55(33), 4559-4563.

[27] Kim, K. Y., Jung, S. H., Lee, J. H., Lee, S. S., & Jung, J. H. (2014). An imidazole-appended p-phenylene-Cu (II) ensemble as a chemoprobe for histidine in biological samples. *Chemical Communications*, 50(96), 15243-15246.

[28] Mamedov, M., Nadtochenko, V., & Semenov, A. (2015). Primary electron transfer processes in photosynthetic reaction centers from oxygenic organisms. *Photosynthesis research*, 125(1-2), 51-63.

[29] Chan, J., Dodani, S. C., & Chang, C. J. (2012). Reaction-based small-molecule fluorescent probes for chemoselective bioimaging. *Nature chemistry*, 4(12), 973-984.

[30] Baki, C. N., & Akkaya, E. U. (2001). Boradiazaindacene-appended calix [4] arene: fluorescence sensing of pH near neutrality. *The Journal of Organic Chemistry*, 4(66), 1512-1513.

[31] de Silva, A. P., Gunaratne, H. N., & Sandanayake, K. S. (1990). A new benzo-annelated cryptand and a derivative with alkali cation-sensitive fluorescence. *Tetrahedron letters*, *31*(36), 5193-5196.

[32] Fabbrizzi, L., Licchelli, M., Pallavicini, P., Perotti, A., & Sacchi, D. (1994). An Anthracene-Based Fluorescent Sensor for Transition Metal Ions. *Angewandte Chemie International Edition in English*, *33*(19), 1975-1977.

[33] Wu, Y., Peng, X., Guo, B., Fan, J., Zhang, Z., Wang, J., ... & Gao, Y. (2005). Boron dipyrromethene fluorophore based fluorescence sensor for the selective

imaging of Zn (II) in living cells. *Organic & biomolecular chemistry*, *3*(8), 1387-1392.

[34] Kim, S. K., Lee, S. H., Lee, J. Y., Lee, J. Y., Bartsch, R. A., & Kim, J. S. (2004). An excimer-based, binuclear, on− off switchable calix [4] crown chemosensor. *Journal of the American Chemical Society*, *126*(50), 16499-16506.

[35] Chan, J., Dodani, S. C., & Chang, C. J. (2012). Reaction-based small-molecule fluorescent probes for chemoselective bioimaging. *Nature chemistry*, *4*(12), 973-984.

[36] Turfan, B., & Akkaya, E. U. (2002). Modulation of boradiazaindacene emission by cation-mediated oxidative PET. *Organic Letters*, *4*(17), 2857-2859.

[37] Valeur, B., & Leray, I. (2000). Design principles of fluorescent molecular sensors for cation recognition. *Coordination Chemistry Reviews*, *205*(1), 3-40.

[38] Hsieh, Y. C., Chir, J. L., Wu, H. H., Guo, C. Q., & Wu, A. T. (2010). Synthesis of a sugar-aza-crown ether-based cavitand as a selective fluorescent chemosensor for Cu2+ ion. *Tetrahedron Letters*, *51*(1), 109-111.

[39] Clapp, A. R., Medintz, I. L., & Mattoussi, H. (2006). Förster resonance energy transfer investigations using quantum-dot fluorophores. *ChemPhysChem*, *7*(1), 47-57.

[40] Sharma, S. K., & Pujari, P. K. (2017). Role of free volume characteristics of polymer matrix in bulk physical properties of polymer nanocomposites: A review of positron annihilation lifetime studies. *Progress in Polymer Science*, *75*, 31-47.

[41] Jeong, Y., & Yoon, J., (2012). Recent progress on fluorescent chemosensors for metal ions. *Inorganica Chimica Acta*, 381, 2-14.

[42] He, G., Zhao, L., Chen, K., Liu, Y. & Zhu, H. (2013). Highly selective and sensitive gold nanoparticle-based colorimetric assay for PO_4^{3-} in aqueous solution. *Talanta* 106, 73–78.

[43] Chen, YC., Lo, KM., Wang, YX. *et al.* A. (2020). sensitive colorimetric probe for detection of the phosphate ion. *Sci Rep* 10, 21215.

[44] Jaffe, H. H., & Miller A.L. (1966). The fates of electronic excitation energy. *Journal of Chemical Education* 43 (9), 469.

[45] Priestley, E.B., & Haug A. (1968). Phosphorescence Spectrum of Pure Crystalline Naphthalene. *Journal of Chemical Physics* 49, 622.

[46] Lim, N. C., Pavlova, S. V., & Brückner, C. (2009). Squaramide hydroxamate-based chemidosimeter responding to iron (III) with a fluorescence intensity increase. *Inorganic chemistry*, *48*(3), 1173-1182.

[47] an, L. J., & Jones, W. E. (2006). A highly selective and sensitive inorganic/organic hybrid polymer fluorescence “turn-on” chemosensory system for iron cations. *Journal of the American Chemical Society*, *128*(21), 6784-6785.

[48] Xu, M., Wu, S., Zeng, F., & Yu, C. (2010). Cyclodextrin supramolecular complex as a water-soluble ratiometric sensor for ferric ion sensing. *Langmuir*, *26*(6), 4529-4534.

[49] Bricks, J. L., Kovalchuk, A., Trieflinger, C., Nofz, M., Büschel, M., Tolmachev, A. I., ... & Rurack, K. (2005). On the development of sensor molecules that display FeIII-amplified fluorescence. *Journal of the American Chemical Society*, *127*(39), 13522-13529.

[50] Li, N., Xu, Q., Xia, X., Lu, J., & Wen, X. (2009). A polymeric chemosensor for Fe^{3+} based on fluorescence quenching of polymer with quinoline derivative in the side chain. *Materials Chemistry and Physics*, *114*(1), 339-343.

[51] Li, J., Wang, Q., Guo, Z., Ma, H., Zhang, Y., Wang, B., Bin, D., Wei, Q. (2016). Highly selective fluorescent chemosensor for detection of Fe^{3+} based on Fe_3O_4@ZnO. *Scientific Reports* 6:23558.

[52] Arulraj et al. (2015) Highly selective and sensitive fluorescent chemosensor for femtomolar detection of silver ion in aqueous medium. *Sensing and Bio-Sensing Research* 6, 19-24.

[53] Weerasinghe, A. J., Schmiesing, C., Varaganti, S., Ramakrishna, G., & Sinn, E. (2010). Single-and multiphoton turn-on fluorescent Fe3+ sensors based on bis (rhodamine). *The Journal of Physical Chemistry B*, *114*(29), 9413-9419.

[54] Li, N., Xu, Q., Xia, X., Lu, J., & Wen, X. (2009). A polymeric chemosensor for Fe3+ based on fluorescence quenching of polymer with quinoline derivative in the side chain. *Materials Chemistry and Physics*, *114*(1), 339-343.

[55] Yi, C., Tian, W., Song, B., Zheng, Y., Qi, Z., Qi, Q., & Sun, Y. (2013). A new turn-off fluorescent chemosensor for iron (III) based on new diphenylfluorenes with phosphonic acid. *Journal of luminescence*, *141*, 15-22.

[56] Zhang, B., Liu, H., Wu, F., Hao, G., Chen, Y., Tan, C., ... & Jiang, Y. (2017). A dual-response quinoline-based fluorescent sensor for the detection of Copper (II) and Iron (III) ions in aqueous medium. *Sensors and Actuators B: Chemical*, *243*, 765-774.

[57] Hu, Z. Q., Gu, Y. Y., Hu, W. Z., Sun, L. L., Zhu, J. H., & Jiang, Y. (2014). A highly selective and sensitive turn-on fluorescent chemosensor based on rhodamine 6G for iron (III). *ChemistryOpen*, *3*(6), 264-268.

[58] Wang, Y., Guo, R., Hou, X., Lei, M., Zhou, Q., & Xu, Z. (2019). Highly Sensitive and Selective Fluorescent Probe for Detection of Fe^{3+} Based on Rhodamine Fluorophore. *Journal of fluorescence*, *29*(3), 645-652.

[59] Cao, X., Zhang, F., Bai, Y., Ding, X., & Sun, W. (2019). A highly selective "turn-on" fluorescent probe for detection of Fe^{3+} in cells. *Journal of fluorescence, 29*(2), 425-434.

[60] Şenkuytu, E., & Okutan, E. Novel probes for selective fluorometric sensing of Fe (II) and Fe (III) based on BODIPY dyes. *Journal of the Turkish Chemical Society Section A: Chemistry*, *6*(2), 207-216.

[61] Li et al. (20156). Colorimetric recognition of Cu^{2+} and fluorescent detection of Hg^{2+} in aqueous media by a dual chemosensor derived from rhodamine B dye with a NS_2 receptor. *Sensors and Actuators B Chemical*, 226, 332-341.

[62] Long, L., Zhou, L., Wang, L., Meng, S., Gong, A., & Zhang, C. (2014). A ratiometric fluorescent probe for iron (III) and its application for detection of iron (III) in human blood serum. *Analytica Chimica Acta*, *812*, 145-151.

[63] Mao, J., He, Q., & Liu, W. (2010). An rhodamine-based fluorescence probe for iron (III) ion determination in aqueous solution. *Talanta*, *80*(5), 2093-2098.

[64] Danjou, P. E., Lyskawa, J., Delattre, F., Becuwe, M., Woisel, P., Ruellan, S., ... & Cazier-Dennin, F. (2012). New fluorescent and electropolymerizable N-azacrown carbazole as a selective probe for iron (III) in aqueous media. *Sensors and Actuators B: Chemical*, *171*, 1022-1028.

[65] Yang, D., Dai, C., Hu, Y., Liu, S., Weng, L., Luo, Z., ... & Wang, L. (2017). A new polymer-based fluorescent chemosensor incorporating propane-1, 3-dione

and 2, 5-diethynylbenzene moieties for detection of copper (II) and iron (III). *Polymers*, *9*(7), 267.

[66] Bordini, J., Calandreli, I., Silva, G. O., Ferreira, K. Q., Leitão-Mazzi, D. P., Espreafico, E. M., & Tfouni, E. (2013). A rhodamine-B-based turn-on fluorescent sensor for biological iron (III). *Inorganic Chemistry Communications*, *35*, 255-259.

[67] Chung, P. K., Liu, S. R., Wang, H. F., & Wu, S. P. (2013). A pyrene-based highly selective turn-on fluorescent chemosensor for iron (iii) ions and its application in living cell imaging. *Journal of fluorescence*, *23*(6), 1139-1145.

[68] Liu, S. R., & Wu, S. P. (2012). New water-soluble highly selective fluorescent chemosensor for Fe (III) ions and its application to living cell imaging. *Sensors and Actuators B: Chemical*, *171*, 1110-1116.

[69] Wang, J., Zhang, D., Liu, Y., Ding, P., Wang, C., Ye, Y., & Zhao, Y. (2014). A N-stablization rhodamine-based fluorescent chemosensor for Fe3+ in aqueous solution and its application in bioimaging. *Sensors and Actuators B: Chemical*, *191*, 344-350.

[70] Liu, J., Xie, Y. Q., Lin, Q., Shi, B. B., Zhang, P., Zhang, Y. M., & Wei, T. B. (2013). Dipodal fluorescent chemosensor for Fe3+ and resultant complex as a chemosensor for fluoride. *Sensors and Actuators B: Chemical, 186,* 657-665.

[71] Turfan, B., & Akkaya, E.U. (2002). Modulation of Boradiazaindacene Emission by Cation-Mediated Oxidative PET. *Organic Letter*, 4, 17, 2857–2859.

[72] Szmacinski, H., & Lakowicz, J.R. (1994). Lifetime-based sensing. In Topics in fluorescence spectroscopy, Vol. 4: Probe design and chemical sensing, pp. 295–334. Ed JR Lakowicz. Plenum Press, New York.

[73] Rettig, W., & Lapouyade, R. (1994). Fluorescence probes based on twisted intramolecular charge transfer (TICT) states and other adiabatic photoreactions. In Topics in fluorescence spectroscopy, Vol. 4: Probe design and chemical sensing, pp. 109–149. Ed JR Lakowicz. Plenum Press, New York.

[74] Kaur et al. (2016). A phenothiazine-based "naked-eye" fluorescent probe for the dual detection of Hg^{2+} and Cu^{2+}: Application as a solid state sensor. *Dyes and Pigments*, 125, 1-7.

[75] Strieth-Kalthoff et al. (2018). Energy transfer catalysis mediated by visible light: principles, applications, directions. *Chem. Soc. Rev.*, 47, 7190-7202.

[76] Dong et al. (2011). Polymer-based fluorescent sensor incorporating 2,2′-bipyridyl and benzo[2,1,3]thiadiazole moieties for Cu^{2+} detection. *Inorganic Chemistry Communications*, 14, 11, 1719-1722.

[77] Sahoo, S. K., Sharma, D., Bera, R. K., Crisponi, G., & Callan, J. F. (2012). Iron (III) selective molecular and supramolecular fluorescent probes. *Chemical Society Reviews*, 41(21), 7195-7227.

[78] Bian, N., Chen, Q., Qiu, X. L., Qi, A. D., & Han, B. H. (2011). Imidazole-bearing tetraphenylethylene: fluorescent probe for metal ions based on AIE feature. *New Journal of Chemistry*, *35*(8), 1667-1671.

[79] Feng, L., Chen, Z., & Wang, D. (2007). Selective sensing of Fe3+ based on fluorescence quenching by 2, 6-bis (benzoxazolyl) pyridine with β-cyclodextrin in neutral aqueous solution. *Spectrochimica Acta Part A: Molecular and Biomolecular Spectroscopy*, *66*(3), 599-603.

[80] Zhou, G., Qian, G., Ma, L., Cheng, Y., Xie, Z., Wang, L., ... & Wang, F. (2005). Polyfluorenes with phosphonate groups in the side chains as chemosensors and electroluminescent materials. *Macromolecules*, *38*(13), 5416-5424.

[81] Li, N., Xu, Q., Xia, X., Lu, J., & Wen, X. (2009). A polymeric chemosensor for Fe^{3+} based on fluorescence quenching of polymer with quinoline derivative in the side chain. *Materials Chemistry and Physics*, *114*(1), 339-343.

[82] Moon, K. S., Yang, Y. K., Ji, S., & Tae, J. (2010). Aminoxy-linked rhodamine hydroxamate as fluorescent chemosensor for Fe^{3+} in aqueous media. *Tetrahedron Letters*, *51*(25), 3290-3293.

[83] Li, P., Zhang, D., Zhang, Y., Lu, W., Wang, W., & Chen, T. (2018). Ultrafast and efficient detection of formaldehyde in aqueous solutions using chitosan-based fluorescent polymers. *ACS sensors*, *3*(11), 2394-2401.

[84] Maity, S., Parshi, N., Prodhan, C., Chaudhuri, K., & Ganguly, J. (2018). Characterization of a fluorescent hydrogel synthesized using chitosan, polyvinyl alcohol and 9-anthraldehyde for the selective detection and discrimination of trace Fe^{3+} and Fe^{2+} in water for live-cell imaging. *Carbohydrate polymers*, *193*, 119-128.

[85] Wang, X., Su, Y., Yang, H., Dong, Z., & Ma, J. (2012). Highly sensitive fluorescence probe based on chitosan nanoparticle for selective detection of Hg^{2+} in water. *Colloids and Surfaces A: Physicochemical and Engineering Aspects*, *402*, 88-93.

[86] Li, M., Xiong, G., Zhang, Y., Yu, X., Cao, Q., & Xiao, H. (2020). Remarkable fluorimetric response and colorimetric sense on the mercury deionization in aqueous solution by a new adsorbent based on chitosan. *European Polymer Journal*, 109663.

[87] Lee, H. M., Kim, M. H., Yoon, Y. I., & Park, W. H. (2017). Fluorescent property of chitosan oligomer and its application as a metal ion sensor. *Marine Drugs*, *15*(4), 105.

[88] Li, Z. A., Lou, X., Yu, H., Li, Z., & Qin, J. (2008). An imidazole-functionalized polyfluorene derivative as sensitive fluorescent probe for metal ions and cyanide. *Macromolecules*, *41*(20), 7433-7439.

[89] Feng, L., Deng, Y., Wang, X., & Liu, M. (2017). Polymer fluorescent probe for Hg (II) with thiophene, benzothiazole and quinoline groups. *Sensors and Actuators B: Chemical*, *245*, 441-447.

[90] Özdemir, E., Thirion, D., & Yavuz, C. T. (2015). Covalent organic polymer framework with C–C bonds as a fluorescent probe for selective iron detection. *RSC advances*, *5*(84), 69010-69015.

[91] Fan, L. J., Zhang, Y., Murphy, C. B., Angell, S. E., Parker, M. F., Flynn, B. R., & Jones Jr, W. E. (2009). Fluorescent conjugated polymer molecular wire chemosensors for transition metal ion recognition and signaling. *Coordination Chemistry Reviews*, *253*(3-4), 410-422.

[92] Huang, H., Wang, K., Tan, W., An, D., Yang, X., Huang, S., ... & Jin, Y. (2004). Design of a Modular-Based Fluorescent Conjugated Polymer for Selective Sensing. *Angewandte Chemie*, *116*(42), 5753-5756.

[93] Choudhury, N., Saha, B., Ruidas, B., & De, P. (2019). Dual-action polymeric probe: turn-on sensing and removal of Hg^{2+}; chemosensor for HSO4–. *ACS Applied Polymer Materials*, 1(3), 461-471.

[94] Ma, B., Zeng, F., Zheng, F., & Wu, S. (2011). A Fluorescence Turn-on Sensor for Iodide Based on a Thymine–HgII–Thymine Complex. *Chemistry–A European Journal*, 17(52), 14844-14850.

[95] Turkewitsch, P., Wandelt, B., Darling, G. D., & Powell, W. S. (1998). Fluorescent functional recognition sites through molecular imprinting. A polymer-based fluorescent chemosensor for aqueous cAMP. *Analytical Chemistry*, 70(10), 2025-2030.

[96] Maity et al. (2018). Characterization of a fluorescent hydrogel synthesized using chitosan, polyvinyl alcohol and 9-anthraldehyde for the selective detection and discrimination of trace Fe^{3+} and Fe^{2+} in water for live-cell imaging. *Carbohyd. Polym*. 193, 119-128.

[97] Fan et al. (2019). A chitosan-based fluorescent hydrogel for selective detection of Fe^{2+} ions in gel-to-sol mode and turn-off fluorescence mode. *Polym. Chem*. 10 5037-5043.

[98] Xiong et al. (2019). Fluorescent chitosan hydrogel for highly and selectively sensing of p-nitrophenol and 2, 4, 6-trinitrophenol. *Carbohydrate Polymers*, 225:115253.

[99] Xiong et al. (2020). A novel coumarin-chitosan fluorescent hydrogel for the selective identification of Fe^{2+} in aqueous systems. *Polym. Chem*.,11, 6066-6072.

[100] Meng et al. (2012). Novel chitosan-based fluorescent materials for the selective detection and adsorption of Fe^{3+} in water and consequent bio-imaging applications. *Talanta*, 97, 456-461.

[101] Pak et al. (2021). Conjugated polymer based fluorescent probes for metal ions. *Coordination Chemistry Reviews*, 433, 213745.

[103] Bialonska, D., Kasimsetty, S. G., Khan, S. I., & Ferreira, D. (2009). Urolithins, intestinal microbial metabolites of pomegranate ellagitannins, exhibit potent antioxidant activity in a cell-based assay. *Journal of Agricultural and Food Chemistry*, 57(21), 10181-10186.

[104] Ji et al. (2013). A Supramolecular Cross-Linked Conjugated Polymer Network for Multiple Fluorescent Sensing. J. Am. Chem. Soc. 135, 1, 74–77.

[105] Cozza, G., Gianoncelli, A., Bonvini, P., Zorzi, E., Pasquale, R., Rosolen, A., ... & Moro, S. (2011). Urolithin as a converging scaffold linking ellagic acid and coumarin analogues: design of potent protein kinase CK2 inhibitors. *ChemMedChem*, *6*(12), 2273-2286.

[106] Tomás-Barberán, F. A., González-Sarrías, A., García-Villalba, R., Núñez-Sánchez, M. A., Selma, M. V., García-Conesa, M. T., & Espín, J. C. (2017). Urolithins, the rescue of “old” metabolites to understand a “new” concept: Metabotypes as a nexus among phenolic metabolism, microbiota dysbiosis, and host health status. *Molecular nutrition & food research*, *61*(1), 1500901.

[107] Gulcan, H. O., Unlu, S., Esiringu, İ., Ercetin, T., Sahin, Y., Oz, D., & Sahin, M. F. (2014). Design, synthesis and biological evaluation of novel 6H-benzo [c] chromen-6-one, and 7, 8, 9, 10-tetrahydro-benzo [c] chromen-6-one derivatives

as potential cholinesterase inhibitors. *Bioorganic & medicinal chemistry*, *22*(19), 5141-5154.

[108] Fallah A, Gülcan HO, Gazi M. (2018). Urolithin B as a simple, selective, fluorescent probe for sensing Iron (III) in semi-aqueous solution. *J. Fluoresc*. 28 (5):1255–1259.

[109] Shi, J., & Zhang, Z. (2020). Synthesis and biological application of a water-soluble fluorescent probe for Fe^{3+} based on sodium benzo [c] chromene-2-sulfonate. *Inorganica Chimica Acta*, 511, 119790.

[110] Sheng et al. (2014). A water-soluble fluorescent probe for Fe(III): Improved selectivity over Cr(III). Sensors and Actuators B: Chemical, 195, 534-539.

[111] Fallah et al. (2020). Urolithin A and B Derivatives as ON-OFF Selective Fluorescent Sensors for Iron (III). *Journal of Fluorescence*, 30:113–120.

[112] Zhang et al. (2017). A dual-response quinoline-based fluorescent sensor for the detection of Copper (II) and Iron (III) ions in aqueous medium. Sensors and Actuators B: Chemical 243, 765-774.

[113] Madhu, P., & Sivakumar, P. (2019). A novel pyridine-pyrazole based selective "turn-off" fluorescent chemosensor for Fe (III) ions. *Journal of Photochemistry and Photobiology A: Chemistry*, 371, 341-348.